A Sublimable Dinuclear Cuprous Complex Showing Selective Luminescence Vapochromism in the Crystalline State

Xing-Wei Chen,[†,⊥] Hua-Li Yuan,[†,⊥] Li-Hua He,[†] Jing-Lin Chen,*[,†,‡,∥] Sui-Jun Liu,[†] He-Rui Wen,[†] Guijiang Zhou,*[,§] Jin-Yun Wang,*[,∥] and Wai-Yeung Wong*[,‡]

[†] *School of Chemistry and Chemical Engineering, Jiangxi University of Science and Technology, Ganzhou 341000, People's Republic of China*

[‡] *Department of Applied Biology and Chemical Technology, The Hong Kong Polytechnic University, Hung Hom, Hong Kong, People's Republic of China*

[§] *MOE Key Laboratory for Nonequilibrium Synthesis and Modulation of Condensed Matter, State Key Laboratory for Mechanical Behavior of Materials, Departement of Chemistry, Faculty of Science, Xi'an Jiaotong University, Xi'an 710049, People's Republic of China*

[∥] *State Key Laboratory of Structural Chemistry, Fujian Institute of Research on the Structure of Matter, Chinese Academy of Sciences, Fuzhou 350002, People's Republic of China*

ABSTRACT: A new sublimable dicopper(I) complex bearing 1,2-bis(diphenylphosphino)ethane and 5-trifluoromethyl-3-(2′-pyridyl)pyrazolate ligands has been designed and synthesized, and its crystalline solvated and non-solvated compounds have also been obtained and investigated. It is shown that only the crystalline solvated compound exhibits reversible and selective luminescence vapochromism, arising from its unique "pyridyl/CH_2Cl_2/pyridyl" organic sandwich-like stacking arrangement revealed by X-ray crystallography, as supported by TDDFT calculations. Additionally, the neutral Cu(I) complex has excellent thermal stability and sublimability, good solid-state luminescence properties, and TADF character, and it is suggested to be a good emitter for vapor-deposited OLEDs.

KEYWORDS

Copper(I) complex; Pyridyl pyrazole; NH-deprotonation; Luminescence; Vapochromism

INTRODUCTION

Luminescence vapochromism, often called vapoluminescence, is of intense interest to chemists and materials scientists due to its potential applications for detection of harmful volatile organic compounds (VOCs) in the environment and the workplace.[1] Vapoluminescent materials are usually characterized by emission wavelength change upon vapors of VOCs. The subsequent reversion to their original emissions is usually achieved upon thermal treatment or placing in air. Emissive Cu(I) complexes have received rapidly increasing attractiveness because of their intriguing luminescence properties including thermally activated delayed fluorescence (TADF) and promising potential for use in various fields,[2] such as detection and sensing,[3] biological labelling,[4] and display visualization devices.[5] However, vapoluminescent Cu(I) complexes are relatively limited.[6] To the best of our knowledge, it has not been reported hitherto that reversible and selective luminescence vapochromism for Cu(I) complexes is achieved by loss/uptake of VOCs.

Non-covalent interactions, including CH···π and halogen···π contacts, when rationally integrated into an appropriate structure, often result in the occurrence of a new phenomenon or functionality.[7] When the assembly displays a triple-decker sandwich structure with VOCs as the middle decker, the VOCs are often lost easily, thus leading to the change of intermolecular interactions. Furthermore, after the VOCs lose, if the layer structure can be well maintained and the missing VOCs can enter readily the layer space again, it is very possible that the assembly with a layer structure becomes a chemical sensor. Hence, inserting the VOCs into a double-deck structure to constitute a new triple-decker structure or constructing a triple-decker structure with the VOCs as the middle decker may be an alternative approach for achieving luminescence vapochromism.

Moreover, it is generally recognized that sublimable neutral complexes are more beneficial to improve the performance of organic light emitting diodes (OLEDs) as compared to cationic ones.[8] However, only several vapor-deposited OLEDs doped with neutral sublimable Cu(I) complexes as the emitters have been reported,[9] because the design of neutral sublimable Cu(I) complexes is not easy and the selection of suitable negative ligands is also narrow. It is expected that 5-

trifluoromethyl-3-(2′-pyridyl) pyrazole is a good candidate, because functional 5-trifluoromethyl-3-(2′-pyridyl)pyrazole has been successfully used to prepare highly efficient Pt(II), Ir(III), and Os(II) luminescent complexes as a mono-anionic chelate through the pyrazole-NH deprotonation.[10] Herein, we describe the synthesis and characterization of a new neutral sublimable dinuclear Cu(I) complex $[\{Cu(pyfpz)\}_2(\mu\text{-dppe})_2]$ (**1**) (pyfpzH = 5-trifluoromethyl-3-(2′-pyridyl)pyrazole; dppe = 1,2-bis(diphenylphosphino)ethane) (Scheme 1). It is shown that only its crystalline solvated compound shows reversible and selective luminescence vapochromism, which is attributed to its peculiar "pyridyl/CH_2Cl_2/pyridyl" organic sandwich-like stacking arrangement. Moreover, it is also suggested that this sublimable Cu(I) complex is a good emitter for vapour-deposited OLEDs due to its high thermal stability and good solid-state luminescence properties.

EXPERIMENTAL SECTION

General Procedures and Materials. All reactions were performed under an inert Ar atmosphere using anhydrous solvents or solvents treated with an appropriate drying reagent. 1,2-Bis(diphenylphosphino)ethane (dppe) was purchased from Aldrich Chemical Co.. $[Cu(CH_3CN)_4](ClO_4)$[11] and 5-trifluoromethyl-3-(2′-pyridyl)pyrazole (pyfpzH)[12] were synthesized by literature procedures.

Caution! *Perchlorate salts are potentially explosive and should be handled carefully in a small amount.*

Preparation of $[\{Cu(pyfpz)\}_2(\mu\text{-dppe})_2]$ (1). A mixture of $[Cu(CH_3CN)_4](ClO_4)$ (26.2 mg, 0.080 mmol) and dppe (31.9 mg, 0.080 mmol) in CH_2Cl_2 (5 mL) was stirred for 15 min at room temperature; pyfpzH (17.1 mg, 0.080 mmol) was added and the mixture was stirred for 30 min to get a light yellow solution. Powdered NaOH (3.6 mg, 0.090 mmol) was then added and this mixture was stirred for another 1 h. After the solvent was evaporated to dryness under reduced pressure, the residue was extracted with 1,2-dichloroethane. The crystalline non-solvated compound **1** was obtained as light yellow crystals by diffusion of *n*-hexane into the above 1,2-dichloroethane solution (39.9 mg, 0.030 mmol, 75%). Anal. Calcd for $C_{70}H_{58}Cu_2F_6N_6P_4$: C, 62.36; H, 4.34; N, 6.23. Found:

C, 62.31; H, 4.37; N, 6.27. Selected IR (KBr, cm^{-1}): 3056w, 1602m, 1531w, 1498m, 1437s, 1380w, 1328w, 1247s, 1138vs, 1101vs, 983m, 779m, 741s, 697s, 513m, 480m.

Preparation of [{Cu(pyfpz)}$_2$(μ-dppe)$_2$]·½CH_2Cl_2 (1·½CH_2Cl_2). The crystalline solvated compound **1**·½CH_2Cl_2 was obtained in 73% yield as light yellow crystals according to the procedure for the crystalline non-solvated compound **1**, followed by diffusion of *n*-hexane into the CH_2Cl_2 solution. Anal. Calcd for $C_{70.5}H_{59}Cu_2F_6N_6P_4Cl$: C, 60.89; H, 4.28; N, 6.04. Found: C, 60.98; H, 4.37; N, 6.15. Selected IR (KBr, cm^{-1}): 3055w, 1601m, 1533w, 1498m, 1437s, 1380w, 1328w, 1246s, 1138vs, 1101vs, 984m, 779m, 742s, 696s, 513m, 481m.

Crystal Structural Determination. Crystal data of **1** and **1**·½CH_2Cl_2 were collected on a Bruker D8 QUEST diffractometer with a graphite-monochromated Mo Kα radiation (λ = 0.71073 Å). Data reduction was performed using Bruker SAINT Software. Intensities were corrected for absorption using SADABS, and the structures were solved by direct methods and refined by full-matrix least-squares technique on F^2 using the SHELXTL software package.[13] The heavy atoms were located from *E*-map and other non-hydrogen atoms were found in subsequent difference Fourier syntheses. All non-hydrogen atoms were refined anisotropically, while hydrogen atoms were geometrically generated with isotropic thermal parameters. The solvent CH_2Cl_2 molecule is symmetrically disordered in **1**·½CH_2Cl_2.

Physical Measurements. ^{1}H and ^{31}P NMR spectra were recorded on Bruker Avance 400 NMR spectrometer. Infrared (IR) spectra were collected on a Bruker Optics ALPHA FT-IR spectrometer using KBr pellets. Elemental analyses (C, H, and N) were conducted on a Perkin Elmer model 240C elemental analyzer. Powder X-ray diffraction (PXRD) data were recorded on an Empyrean (PANalytical B.V.) diffractometer for a Cu-target tube and a graphite monochromator. Simulation of the PXRD patterns was carried out by using the single-crystal structural data and diffraction-crystal module of the Mercury (Hg) program version 3.0 available free of charge via the Internet at http://www.iucr.org. Thermogravimetric analysis (TGA) measurements were performed on a Perkin Elmer Pyris Diamond TG/DTA 6300 instrument under a nitrogen gas atmosphere at a heating rate

of 15 °C min^{-1}. The photoluminescence properties in CH_2Cl_2 and in the solid state were measured on an Edinburgh analytical instrument (F900 fluorescence spectrometer) with a thermoelectrically cooled Hamamatsu R3809 photomultiplier tube. The emission quantum yields (Φ_{em}) in CH_2Cl_2 at ambient temperature were calculated by $\Phi_s = \Phi_r(B_r/B_s)(n_r/n_s)^2(D_s/D_r)$ using fluorescein in H_2O as the standard ($\Phi_{em} = 0.79$), where the subscripts "r" and "s" denote the reference standard and the sample solution, respectively, and n, D and Φ are the refractive index of the solvents, the integrated intensity and the emission quantum yield, respectively.[14] The quantity B is calculated by $B = 1-10^{-AL}$, where A is the absorbance at the excitation wavelength and L is the optical path length. An integrating sphere (Lab sphere) was used to measure the emission quantum yield in the solid state.

Computational Methodology. All the calculations were carried out by using the Gaussian 09 program[15] to analyze the electronic structures and photophysical properties of complex **1**. Firstly, the restricted density functional theory (DFT)[16] method with the Becke Three-Parameter Hybrid Functional B3LYP using the non-local correlation provided by the LYP expression and VWN functional III for local correlation was used to optimize the ground-state (S_0) structure of complex **1** without symmetry constraint. The initial structure was extracted from the crystallographically determined geometry. During the optimization processes, the convergent values of maximum force, root-mean-square (RMS) force, maximum displacement and RMS displacement were set by default. To analyze the absorption and emission transition properties, eighty singlet and six triplet excited states for **1** in CH_2Cl_2 media were calculated by the time-dependent DFT (TDDFT)[17] method at the same functional used in the geometrical optimization based on the optimized ground-state S_0 structure. The solvent effects in CH_2Cl_2 media were taken into account by performing the self-consistent reaction field (SCRF) calculations using the polarizable continuum model method (PCM).[18] Moreover, to analyze the influence of CH_2Cl_2 solvate molecules on the electronic structures of **1**·½CH_2Cl_2 in the solid state, the neighboring two parallel [{Cu(pyfpz)}$_2$(μ-dppe)$_2$] molecule models without and with a CH_2Cl_2 molecule were, respectively, selected to perform the TDDFT calculations. In these calculations, the Stuttgart-Dresden basis set[19] consisting of the

effective core potentials (ECP) was employed for the Cu and P atoms, and 6-31G(p,d) basis set[20] for the remaining atoms were used. Visualization of the frontier molecular orbitals was performed by GaussView. Ros & Schuit method (C-squared population analysis method, SCPA)[21] is supported to analyze the partition orbital composition by using Multiwfn 3.3.8 program.[22]

OLED Fabrication and Measurements. All the OLEDs were made by the vacuum deposition method. The indium tin oxide (ITO) glass substrates were pre-cleaned with ethanol, acetone, and deionized water under an ultrasonic bath, and then treated with UV-ozone for 30 min. After a 40 nm thick 4,4′-bis[*N*-(1-naphthyl)-*N*-phenylamino]biphenyl (NPB) layer was deposited on the surface of the pre-treated ITO glass, the Cu(I) phosphor and 4,4′-bis(9-carbazolyl)-1,1′-biphenyl (CBP) host were co-evaporated to form a 40 nm thick emitting layer. Then, 1,3,5-tris(*N*-phenylbenzimidazol-2-yl)benzene (TPBi) (45 nm), LiF (1 nm), and a 100 nm thick Al cathode were successively evaporated at a base pressure of less than 10^{-6} Torr. The electroluminescence spectra and CIE coordinates of the OLEDs were measured with a PR650 spectra colorimeter. The current density–voltage–luminance curves of the OLEDs were recorded using a Keithley 2400/2000 source meter and the luminance was measured using a PR650 SpectraScan spectrometer. All the experiments and measurements were carried out at room temperature under ambient conditions.

RESULTS AND DISCUSSION

Synthesis and characterization. Treatment of $[Cu(CH_3CN)_4](ClO_4)$ in CH_2Cl_2 with an equimolar amount of 1,2-bis(diphenylphosphino)ethane (dppe) and 5-trifluoromethyl-3-(2′-pyridyl) pyrazole (pyfpzH) in the presence of NaOH gave the expected target product $[\{Cu(pyfpz)\}_2(\mu\text{-dppe})_2]$ (**1**) (Scheme 1). Its crystalline solvated compound **1**·½CH_2Cl_2 was first obtained as light yellow crystals by diffusion of *n*-hexane into a CH_2Cl_2-containing solution, and the crystal structure was revealed by single-crystal X-ray diffraction analysis (*vide infra*). Interestingly, it is noted that the crystalline solvated compound **1**·½CH_2Cl_2 shows luminescence vapochromism to CH_2Cl_2 vapor. To find out the relationship between the crystalline structure and the CH_2Cl_2-selective luminescence

vapochromism, it is extremely important and necessary to get the crystal structure of compound **1**·½CH_2Cl_2 after loss of CH_2Cl_2. However, unfortunately, all attempts including placing the crystals of **1**·½CH_2Cl_2 in air for several months or directly thermal treatment in the oven of 100 °C for a dozen of days were consistently in vain. As an alternative, we very much hope to obtain the crystal structure of complex **1** without CH_2Cl_2 by other approaches including crystallization. Fortunately, the crystalline non-solvated compound **1** was successfully afforded as light yellow crystals by diffusion of *n*-hexane into a 1,2-dichloroethane, chloroform, 1,2-dichloroethane-acetone, or chloroform-acetone solution without CH_2Cl_2, and its crystal structure was determined successfully by single-crystal X-ray structural analysis (*vide infra*). Different from the crystalline solvated compound **1**·½CH_2Cl_2, the crystalline non-solvated compound **1** does not display luminescence vapochromism to common organic vapors including CH_2Cl_2. The sample purities of the two crystalline compounds **1** and **1**·½CH_2Cl_2 are confirmed by their element analyses and powder X-ray diffractions (*vide infra*). The two crystalline compounds **1** and **1**·½CH_2Cl_2 are soluble in chlorinated solvents such as chloroform, dichloromethane, and 1,2-dichloroethane, but insoluble in other organic solvents including benzene, toluene, acetonitrile, methanol, ethanol, and DMSO. The IR absorption spectra are nearly identical for crystalline **1** and **1**·½CH_2Cl_2 (Figures S1 and S2), perhaps because the C−H and Cl−C−Cl vibration signals from CH_2Cl_2 that is the only difference are overlaid by those from pyfpz and dppe (Figures S3 and S4). In addition, the two crystalline compounds **1** and **1**·½CH_2Cl_2 are considerably air-stable in the solid state despite slow removal of CH_2Cl_2 for **1**·½CH_2Cl_2, whereas the isomerization is clearly observed in solution as soon as the two crystalline compounds **1** and **1**·½CH_2Cl_2 are dissolved (even in a non-coordinating solvent such as CH_2Cl_2), as supported by ^{1}H NMR spectra of **1**·½CH_2Cl_2 (Figures S5, S7 and S9). However, similar isomerization behavior has not been observed in previously reported pyfpzH-based dinuclear Cu(I) derivative of 1,4-bis(diphenylphosphino)butane (dppb) with a longer methylene chain *versus* dppe, i.e. [{Cu(pyfpzH)}$_2$(μ-dppb)$_2$](ClO_4)$_2$,[23] suggesting that the diphosphine ligand has a significant influence on the solution stability of this type of dinuclear Cu(I) heteroleptic complexes. The

methylene (CH_2) groups of dppe show three triplet peaks in the ^{1}H NMR spectra of **1**·½CH_2Cl_2 (Figures S5, S7 and S9), together with a broad singlet peak presented in the ^{31}P NMR spectra (δ = −7.93~−7.49 ppm, Figures S6, S8 and S10), implying that two possible isomers exist in solution and the molar ratio of the two ones (observed, 1.1−2.1) depends on the solvent nature and the storage time of solution. The integral ratio of the CH_2 proton signals from CH_2Cl_2 and dppe in the ^{1}H NMR spectra (Figures S5, S7 and S9) is approximately 1/8, which is in accord well with the CH_2Cl_2 and dppe molar ratio (1/4) of **1**·½CH_2Cl_2. In the light of the variable-temperature ^{1}H and ^{31}P NMR spectra (Figures S11 and S12) of **1**·½CH_2Cl_2 in CD_2Cl_2, this isomerization most likely belongs to an equilibrium of two possible species [{Cu(pyfpz)}$_2$(μ-dppe)$_2$] and [Cu(pyfpz)(dppe)] (Figure S13), which originates from a collaborative rearrangement of the two dppe ligands involving decoordination of one P atom from one Cu atom and recoordination to the other Cu atom. On the basis of the assumption, one (2.47 ppm) of the three triplets from dppe (Figure S5), which can be further split into two triplets at low temperature such as 238 and 218 K (Figure S11), can be assigned to the monomer [Cu(pyfpz)(dppe)], while the other two ones (3.59 and 1.90 ppm) are almost the same at room temperature and at low temperature (Figure S11) and can originate from the dimer [{Cu(pyfpz)}$_2$(μ-dppe)$_2$], which is somewhat similar to the multiple peak (2.51−2.49 ppm, 8H, C*H*$_2$-dppe) observed in [Cu$_2${2-(2-*tert*-butyl-2*H*-tetrazol-5-yl)pyridine}$_2$(dppe)$_2$][BF_4]$_2$[2m] and can be caused by weak intramolecular C−H···N^{pz} contacts between the dppe-C*H*$_2$ and pyrazolate groups (CH···N^{pz}, 2.646−2.916 Å, Figure S14) revealed by X-ray crystallography of **1**.

The exact structures of two crystalline compounds **1** and **1**·½CH_2Cl_2 were established by X-ray crystallography. Their crystallographic data and structure refine details are summarized in Table 1, and selected bond lengths and angles are listed in Table 2. As depicted in Figures 1 and S15, the two crystalline compounds **1** and **1**·½CH_2Cl_2 all have a {Cu$_2$(μ-dppe)$_2$} framework with the two Cu(I) atoms doubly linked by two dppe bridges to form an eclipsed boat-chair-boat conformation of a ten-membered $Cu_2P_4C_4$ ring,[2m] and each Cu(I) atom is located in a highly distorted tetrahedral N_2P_2 configuration formed by two N donors of the 3-(2′-pyridyl)pyrazolate fragment and two P

atoms from two dppe bridging ligands, where pyfpz adopts a mono-anionic chelating fashion with the pyrazole-NH deprotonation, as supported by no pyrazolyl-NH proton signal observed in the ^{1}H NMR spectra (Figures S5, S7 and S9). The pyfpz ligand gives an unsymmetrical chelating mode with the Cu−$N_{pyridyl}$ bonds (2.100−2.119 Å) being much longer than the Cu−$N_{pyrazolate}$ ones (2.011−2.039 Å), indicative of an influence of the negative charge of the monoanionic pyrazolate.[23] For the crystalline solvated compound **1**·½CH_2Cl_2, it is noted that two pyfpz chelates of each [{Cu(pyfpz)}$_2$(μ-dppe)$_2$] molecule are parallel with two pyfpz chelates from two neighbouring [{Cu(pyfpz)}$_2$(μ-dppe)$_2$], respectively, and one CH_2Cl_2 solvent molecule is sandwiched between two parallel pyridyl rings (the distance of two pyridyl ring centroids is 7.534 Å, suggesting no π···π interactions between the two pyridyl rings), constituting one-dimensional "pyridyl/CH_2Cl_2/pyridyl" organic sandwich-like stacking arrangement through weak intermolecular CH···π (CH···π, 2.879 and 3.051 Å; C···π, 3.691 and 3.784 Å) and Cl···π (3.693 Å) interactions (Figure 2).[24] However, similar layer stacking arrangement is not observed in the crystalline non-solvated compound **1** (the distance of two pyridyl ring centroids is 9.359 Å, implying no π···π interactions between the two pyridyl rings) (Figure 3). Supramolecular packing of **1** is completed cooperatively by weak F···H (2.602 and 2.667 Å) and H···H (2.327 and 2.397 Å) intermolecular contacts (Figures S16 and S17), whereas that of **1**·½CH_2Cl_2 is achieved by weak Cl···H (2.927 Å) and CH^{ph}···π^{pz} (~2.791 Å) intermolecular interactions (Figures S18 and S19).[25] The powder X-ray diffractions reveal that all the measured diffraction peaks of the two crystalline compounds **1** and **1**·½CH_2Cl_2 (Figures 4a and 4e) are reasonable and consistent with those (Figures 4b and 4f) calculated from their single-crystal X-ray diffraction data, indicating the purity of the two crystalline samples. Moreover, no new diffraction peaks appear in the fully desolvated sample of **1**·½CH_2Cl_2 (Figure 4d), which is more similar to **1** (Figure 4a) than **1**·½CH_2Cl_2 (Figure 4e), and all the observed diffraction peaks of the fully desolvated sample of **1**·½CH_2Cl_2 after regaining CH_2Cl_2 (Figure 4c) are in good accordance with those of **1**·½CH_2Cl_2 (Figure 4e), implying that no new crystalline phase occurs during the desolvated process and the whole cycle is completely reversible. Thus, it can be believed that the

formation of the "pyridyl/CH_2Cl_2/pyridyl" organic sandwich-like stacking arrangement, together with CH_2Cl_2 being able to move freely in and out of the resulting layer space, may be the main causes of **1**·½CH_2Cl_2 exhibiting reversible luminescence vapochromism to only CH_2Cl_2 vapor.

The crystalline solvated compound **1**·½CH_2Cl_2 is light yellow block crystals (Figure 5a). Under UV lamp irradiation at 365 nm, a yellow emission is clearly observed at room temperature (Figure 5c). When the block crystalline solvated sample is exposed to air, its luminescence color changes slowly from yellow to cyan (Figure 5d), whereas there is no observable change of its surface color (Figure 5b). Upon exposure of the fully desolvated block crystalline sample to CH_2Cl_2 vapor, its luminescence color can come slowly back from the cyan to the original yellow. This indicates that the luminescence color change of the block crystalline solvated sample is responsive to CH_2Cl_2 vapor and is completely reversible. For the block crystalline solvated sample, the inter-conversion of the yellow and cyan two luminescence colors is relatively slow and takes several days. However, when the block crystalline solvated sample is ground into the fine powder (Figures 5e and 5f), the reciprocal transformation of two luminescence colors can be finished quickly in less than 12 seconds (Figures 5g and 5h). When the block and powder samples of **1**·½CH_2Cl_2 are exposed to other organic vapors, such as chloroform, 1,2-dichloroethane, tetrahydrofuran, acetonitrile, ethyl acetate, acetone, methanol, ethanol, etc., the luminescence vapochromism cannot be observed, indicative of its high selectivity to CH_2Cl_2 vapor. Surprisingly, the block and powder samples of the crystalline non-solvated compound **1** cannot exhibit luminescent vapochromism to common VOC vapors including CH_2Cl_2. This implies that the selective luminescence vapochromism of **1**·½CH_2Cl_2 is closely related to its especial "pyridyl/CH_2Cl_2/pyridyl" sandwich-like stacking arrangement and weak interactions between CH_2Cl_2 and [{Cu(pyfpz)}$_2$(μ-dppe)$_2$] (Figure 2).

In addition, the thermodynamic properties of two crystalline compounds **1** and **1**·½CH_2Cl_2 and the fully desolvated sample of **1**·½CH_2Cl_2 were also studied. As depicted in Figure 6, the crystalline non-solvated compound **1** and the completely desolvated sample of **1**·½CH_2Cl_2 are stable up to ~310 °C and then sublimes directly without any appreciable decomposition, indicating their high

thermal stability, excellent sublimability, and no solvate molecules existing in their crystal lattices. For the crystalline solvated compound **1**·½CH_2Cl_2, a small weight loss of *ca.* 3.5% is observed in the 130−173 °C region, which is in good agreement with the calculated value corresponding to the loss of half of a co-crystallized CH_2Cl_2 per formula unit (3.1%) revealed by single-crystal X-ray structural analysis of **1**·½CH_2Cl_2. Considering the low boiling point of CH_2Cl_2, this suggests the higher thermal stability of CH_2Cl_2 in **1**·½CH_2Cl_2, as supported by the presence of weak interactions between CH_2Cl_2 and [{Cu(pyfpz)}$_2$(μ-dppe)$_2$] in the crystal lattice (Figure 2).

Photophysical Properties. As shown in Figure 7, in CH_2Cl_2, the pyfpzH ligand displays two broad absorption bands at λ_{max} = 248 and 282 nm, attributable to spin allowed $^1\pi\pi^*$ transitions, while its Cu(I)-dppe complex **1** also exhibits two broad absorption peaks (λ_{max} = 255 and 306 nm, $\varepsilon > 10^4$ M^{-1} cm^{-1}) in the UV region (<330 nm), assigned as the ligand-centered transitions of both pyfpz and dppe ligands, which are slightly red-shifted, due to the more-extended π-conjugation, relative to the free pyfpzH. In addition, similar to previously reported pyfpzH-based Cu(I)-dppb complex,[23] due to the influence of a strong electron-withdrawing CF_3, only a relatively weak low-energy absorption is observed as a shoulder ranging from 330 to 400 nm, which is distinguished from the absorptions observed as a broad peak in previously reported 3-(2′-pyridyl)pyrazole-based Cu(I)-dppb complexes.[23]

As depicted in Figure 8, complex **1** shows at ambient temperature a very feeble green emission (λ_{max} ≈ 539 nm, Φ < 0.01) in CH_2Cl_2 and a moderate emission (λ_{max} = 523 nm) with the quantum yield of 0.17 and the lifetime of 14.7 μs in PMMA (4 wt%), attributed to fast structural relaxation in solution,[26] as supported by the fact that its crystalline compounds **1** and **1**·½CH_2Cl_2 all show strong solid-state emissions (Φ > 0.69) for the retardation of structural relaxation in the solid state.[27] As shown in Figure 9, at room temperature, the crystalline non-solvated compound **1** exhibits a broad and unstructured emission band centred at 493 nm, with the quantum yield of 0.71 and the lifetime of 39.0 μs. Also, the crystalline solvated compound **1**·½CH_2Cl_2 displays an unstructured emission profile, maximized at 518 nm with the quantum yield of 0.69 and the lifetime of 30.2 μs, and nearly

identical luminescence properties reappear in compound **1**·½CH_2Cl_2 after regaining CH_2Cl_2, indicating that the loss and uptake of CH_2Cl_2 are completely reversible for the crystalline solvated compound **1**·½CH_2Cl_2. The crystalline solvated compound **1**·½CH_2Cl_2 (λ_{max} = 518 nm) shows an emission with a lower energy, compared to the crystalline non-solvated compound **1** (λ_{max} = 493 nm), perhaps attributed to the influence of weak interactions between CH_2Cl_2 and [{Cu(pyfpz)}$_2$(μ-dppe)$_2$] revealed by X-ray crystallography of **1**·½CH_2Cl_2 (Figure 2), decreasing the LUMO level basically localized on pyfpz and, hence, leading to a narrower HOMO−LUMO gap and an emission with lower energy, as supported by TDDFT calculations of **1**·½CH_2Cl_2 before and after loss of CH_2Cl_2 (*vide infra*). In addition, no appreciable emission spectral changes including the quantum yield and lifetime are observed for crystalline non-solvated compound **1** upon exposure to air for about two months (Figure S20), whereas a remarkable emission spectral change can be clearly observed for crystalline solvated compound **1**·½CH_2Cl_2 upon exposure to air for some time (Figure S21), with a maximum spectral blue shift of *ca.* 25 nm, attributed to the loss of crystalline CH_2Cl_2 solvent molecules.

Upon cooling to 77 K, the crystalline non-solvated compound **1** gives a broad emission band with a maximum at 509 nm (Figure 9d), which is red-shifted by 16 nm, relative to that (λ_{max} = 493 nm) at ambient temperature, indicating that the observed emission may result from two interconvertible excited states in thermal equilibrium. To confirm this assumption, the luminescence lifetimes of crystalline non-solvated compound **1** were investigated in the temperature range 50−350 K and shown in Figure 10. It is noted that the observed emission lifetime (τ_{obs}) decreased drastically from 164 μs at 50 K to 24 μs at 350 K. At low temperature such as 77 or 50 K, its population is dominantly frozen in the triplet state and hence the emissive state can be ascribed to pure T_1 state. With temperature increasing, the population of the upper lying S_1 state appears and increases gradually. At ambient temperature, the observed emission may originate principally from the S_1 state, which is significantly populated via an effective up-conversion from the lower lying T_1 state. Assuming a fast thermal equilibrium existing between the S_1 and T_1 emitting states, the observed

emission lifetime (τ_{obs}) can be descripted as follows: $\tau(\mathrm{obs}) = \dfrac{1+\frac{1}{3}\exp\left(-\frac{\Delta E_{ST}}{k_B T}\right)}{\frac{1}{\tau(T_1)}+\frac{1}{3\tau(S_1)}\exp\left(-\frac{\Delta E_{ST}}{k_B T}\right)}$ (1).

An excellent fit to the experimental data in 50−350 K was obtained and depicted in Figure 10 with the values of $\tau(S_1)$ = 420 ns, $\tau(T_1)$ = 160 μs, and ΔE_{ST} = 0.097 eV (780 cm^{-1}) from equation 1. Actually, a small singlet–triplet energy gap ΔE_{ST} is essential to facilitate an effective up-conversion and yield a room-temperature emission dominated by thermally activated delayed fluorescence (TADF), which was often observed in luminescent cuprous complexes.[9g,28]

Theoretical Investigations. To understand the electronic transition properties of the 3-(2′-pyridyl)pyrazole-based dinuclear Cu(I) complex, time-dependent density functional theory (TDDFT) was used to model electronic absorption spectra of **1** in CH_2Cl_2 using the PCM model. The frontier molecular orbitals involved in low-energy electronic absorption transitions are shown in Figure 11. The calculated absorption spectra, absorption transition properties, and frontier molecular orbital compositions are given in the Supporting Information (Tables S1–S2 and Figures S22–S23).

As shown in Table S1 and Figures 11 and S23, the LUMO and LUMO+1 of **1** are basically localized on pyfpz (90.26 and 91.37%), while the HOMO and HOMO-1 mainly reside on Cu(3d) (41.87 and 41.78%), dppe (46.63 and 46.78%), and pyfpz (11.50 and 11.43%). Thus the calculated low-energy absorption at 350 nm dominated by the HOMO→LUMO+1 and HOMO-1→LUMO transitions (Table S2), which is in good agreement with the experimentally measured value (λ_{max} = 355 nm), is a mixed ^{1}LLCT/^{1}MLCT/^{1}IL (dppe/Cu(3d)/pyfpz→pyfpz) process.

The luminescence properties of **1** in CH_2Cl_2 media were also investigated by TDDFT/B3LYP calculations. As depicted in Table S2, the calculated lowest-energy triplet emissive state is largely from the HOMO-2→LUMO (41%) and HOMO-3→LUMO+1 (40%) transitions. It can be seen from Table S1 that the HOMO-2 and HOMO-3 are uniformly distributed on Cu(3d) (58.58 and 59.56%), pyfpz (30.72 and 30.61%), and dppe (10.70 and 9.83%). Thus the lowest-energy emission can be attributed to a mixed ^{3}MLCT/^{3}IL state. It is evident that the calculated ΔE_{ST} value (0.22 eV,

1770 cm^{-1}) allows for thermal equilibrium between the S_1 and T_1 emitting states, which is in good agreement with the experimentally obtained ΔE_{ST} one (0.097 eV, 780 cm^{-1}) based on the emission lifetime dependence on temperature and can be thought to be theoretical support for TADF.

Moreover, to analyze the influence of CH_2Cl_2 solvate molecules on the electronic structures of crystalline **1**·½CH_2Cl_2, TDDFT calculations of neighboring two parallel [{Cu(pyfpz)}$_2$(μ-dppe)$_2$] molecules model without and with a CH_2Cl_2 molecule were performed. As shown in Figure 12, the calculated HOMO–LUMO energy gap (3.91 eV) based on the model with a CH_2Cl_2 molecule is smaller than the calculated value (3.99 eV) based on that without a CH_2Cl_2 molecule, which is in good agreement with the sequence of the experimentally measured emission energies of crystalline compounds **1**·½CH_2Cl_2 (λ_{max} = 518 nm) and **1** (λ_{max} = 493 nm) at ambient temperature.

Electroluminescence Properties. Since complex **1** possesses excellent sublimability and thermal stability and good solid-state photoluminescence properties, which are critical for successful OLED fabrication by vapor deposition, its crystalline non-solvated compound **1** without CH_2Cl_2 solvate molecules is chosen as the emitter. The multilayer devices of the configuration of ITO/NPB (40 nm)/CBP:**1** (40 nm)/TPBI (45 nm)/LiF (1 nm)/Al (100 nm) were prepared, where the abbreviations NPB, CBP, and TPBI stand for 4,4'-bis(*N*-(1-naphthyl)-*N*-phenylamino)biphenyl, 4,4′-bis(9-carbazolyl)-1,1′-biphenyl, and 1,3,5-tris(*N*-phenylbenzimidazol-2-yl)benzene, and the doping concentrations of **1** are 4 wt%, 6 wt%, and 8 wt%, respectively. Table 3 summarizes the selected performance data of these OLEDs, while the current density–voltage–luminance characteristics and electroluminescence efficiency–luminance curves of these OLEDs are presented in Figures 14 and 15. For all doping concentrations, the devices all emit strong electroluminescence and exhibit a relatively low turn-on voltage ($V_{turn\text{-}on}$) of ~4.0 V, and the device with 6 wt% doping concentration shows a maximum external quantum efficiency (η_{ext}) of 7.5%, a maximum current efficiency (η_L) of 15.9 cd A^{-1}, and a maximum power efficiency (η_P) of 12.9 lm W^{-1}. Compared to the solid-state photoluminescence spectra (Figure 9) of crystalline non-solvated compound **1**, it is noted that the electroluminescence spectra of these OLEDs have an extra shoulder appearing at *ca.* 436 nm

(Figure 13), which can be attributed to the CBP host, suggesting that the CBP is not an appropriate host because it cannot transfer the obtained energy effectively to the emissive dopant **1**. Although the performances of these OLEDs have not been well optimized, there is no doubt that the Cu(I) complex **1** is still believed to be a good emitter for vapor-deposited OLEDs.

CONCLUSIONS

We have designed and synthesized a new sublimable dinuclear Cu(I) complex possessing 1,2-bis(diphenylphosphino)ethane and NH-deprotonated 5-trifluoromethyl-3-(2′-pyridyl)pyrazole, and have obtained and investigated its crystalline solvated and non-solvated compounds. It is shown that the crystalline solvated compound displays reversible and selective luminescence vapochromism, which cannot be presented in the crystalline non-solvated compound. As revealed by X-ray crystallography, the reversible and selective luminescence vapochromism is closely associated with the particular "pyridyl/CH_2Cl_2/pyridyl" organic sandwich-like stacking arrangement, as supported by TDDFT analyses. In addition, the neutral dicopper(I) complex exhibits high thermal stability and excellent sublimability and good solid-state luminescence properties with TADF character, and it is suggested to be a good emitter for vapor-deposited OLEDs. The findings presented herein provide a new insight into the design and synthesis of highly efficient vapor-responsive luminescence materials and emitting materials used in vapor-deposited OLEDs.

ASSOCIATED CONTENT

Supporting Information

The Supporting Information is available free of charge on the ACS Publications website at http://pubs.acs.org. The crystallographic data of **1** and **1**·½CH_2Cl_2 (CIF file). Tables and figures regarding the TDDFT calculations and characterization data of **1** and **1**·½CH_2Cl_2 (PDF file).

Accession Codes

CCDC 1815617–1815618 contain the supplementary crystallographic data for this paper

(crystallographic data for **1** and **1**·½CH_2Cl_2). These data can be obtained free of charge via the Internet (www.ccdc.cam.ac.uk/data_request/cif), by E-mail (data_request@ccdc.cam.ac.uk), or by contacting The Cambridge Crystallographic Data Centre, 12 Union Road, Cambridge CB21EZ, UK (fax: +44 1223 336033).

AUTHOR INFORMATION

Corresponding Authors

*E-mail: gzchenjinglin@126.com (J.-L. Chen)

*E-mail: wai-yeung.wong@polyu.edu.hk (W.-Y. Wong)

*E-mail: zhougj@mail.xjtu.edu.cn (G. Zhou)

*E-mail: jy_wang@fjirsm.ac.cn (J.-Y. Wang)

Author Contributions

$^{\perp}$ X.-W.C. and H.-L.Y. contributed equally to this work.

Notes

The authors declare no competing financial interest.

ACKNOWLEDGMENT

The work was supported by the National Natural Science Foundation of China (No. 21861018, 21561013 and 21761012), Jiangxi Provincal Academic and Technical Leaders of the Main Disciplines (No. 20182BCB22010), the Natural Science Foundation of Jiangxi Province of China (No. 20192ACBL20013, 20171BAB203005, 20192BAB203001 and 20171BCB23066), the Foundation of State Key Laboratory of Structural Chemistry (No. 20180019), the Program of Ganzhou Science and Technology Innovation Talents, and the Program for Qingjiang Excellent Young Talents of Jiangxi University of Science and Technology. W.-Y.W. thanks The Hong Kong Polytechnic University (1-ZE1C) and Ms Clarea Au (847S) for financial support.

REFERENCES

(1) (*a*) Albrecht, M.; Lutz, M.; Spek, A. L.; van Koten, G. Organoplatinum crystals for gas-triggered switches. *Nature* **2000**, *406*, 970−974. (*b*) Buss, C. E.; Mann, K. R. Synthesis and Characterization of Pt(CN-*p*-$(C_2H_5)C_6H_4)_2(CN)_2$, a Crystalline Vapoluminescent Compound That Detects Vapor-Phase Aromatic Hydrocarbons. *J. Am. Chem. Soc.* **2002**, *124*, 1031−1039. (*c*) Zhang, X.; Li, B.; Chen, Z.-H.; Chen, Z.-N. Luminescence vapochromism in solid materials based on metal complexes for detection of volatile organic compounds (VOCs). *J. Mater. Chem.* **2012**, *22*, 11427−11441. (*d*) Wenger, O. S. Vapochromism in Organometallic and Coordination Complexes: Chemical Sensors for Volatile Organic Compounds. *Chem. Rev.* **2013**, *113*, 3686−3733.

(2) (*a*) Ford, P. C.; Cariati, E.; Bourassa, J. Photoluminescence Properties of Multinuclear Copper(I) Compounds. *Chem. Rev.* **1999**, *99*, 3625−3647. (*b*) Armaroli, N.; Accorsi, G.; Cardinali, F.; Listorti, A. Photochemistry and Photophysical of Coordination Compounds: Copper. *Top. Curr. Chem*. **2007**, *280*, 69−115. (*c*) Barbieri, A.; Accorsi, G.; Armaroli, N. Luminescent complexes beyond the platinum group: the d^{10} avenue. *Chem. Commun*. **2008**, 2185−2193. (*d*) Yam, V. W.-W.; Au, V. K.-M.; Leung, S. Y.-L. Light-Emitting Self-Assembled Materials Based on d^8 and d^{10} Transition Metal Complexes. *Chem. Rev.* **2015**, *115*, 7589−7728. (*e*) Bizzarri, C.; Spuling, E.; Knoll, D. M.; Volz, D.; Bräse, S. Sustainable metal complexes for organic light-emitting diodes (OLEDs). *Coord. Chem. Rev.* **2018**, *373*, 49−82. (*f*) Dias, H. V. R.; Diyabalanage, H. V. K.; Eldabaja, M. G.; Elbjeirami, O.; Rawashdeh-Omary, M. A.; Omary, M. A. Brightly Phosphorescent Trinuclear Copper(I) Complexes of Pyrazolates: Substituent Effects on the Supramolecular Structure and Photophysics. *J. Am. Chem. Soc.* **2005**, *127*, 7489−7501. (*g*) Nishikawa, M.; Nomoto, K.; Kume, S.; Inoue, K.; Sakai, M.; Fujii, M.; Nishihara, H. Dual Emission Caused by Ring Inversion Isomerization of a 4-Methyl-2-pyridyl-pyrimidine Copper(I) Complex. *J. Am. Chem. Soc*. **2010**, *132*, 9579−9581. (*h*) Lotito, K. J.; Peters, J. C. Efficient luminescence from easily prepared three-coordinate copper(I)

arylamidophosphines. *Chem. Commun*. **2010**, *46*, 3690−3692. (*i*) Manbeck, G. F.; Brennessel, W. W.; Eisenberg, R. Photoluminescent Copper(I) Complexes with Amido-Triazolato Ligands. *Inorg. Chem*. **2011**, *50*, 3431−3441. (*j*) Crestani, M. G.; Manbeck, G. F.; Brennessel, W. W.; McCormick, T. M.; Eisenberg, R. Synthesis and Characterization of Neutral Luminescent Diphosphine Pyrrole and Indole-Aldimine Copper(I) Complexes. *Inorg. Chem*. **2011**, *50*, 7172−7188. (*k*) Li, J.-C.; Li, H.-X.; Li, H.-Y.; Gong, W.-J.; Lang, J.-P. Ligand Coordination Site-Directed Assembly of Copper(I) Iodide Complexes of ((Pyridyl)-1-pyrazolyl)pyridine. *Cryst. Growth Des.* **2016**, *16*, 1617−1625. (*l*) Chen, J.-L.; Zeng, X.-H.; Luo, Y.-S.; Wang, W.-M.; He, L.-H.; Liu, S.-J.; Wen, H.-R.; Huang, S.; Liu, L.; Wong, W.-Y. Synthesis, structure, and photophysics of copper(I) triphenylphosphine complexes with functionalized 3-(2′-pyrimidinyl)-1,2,4-triazole ligands. *Dalton Trans.* **2017**, *46*, 13077−13087. (*m*) Femoni, C.; Muzzioli, S.; Palazzi, A.; Stagni, S.; Zacchini, S.; Monti, F.; Accorsi, G.; Bolognesi, M.; Armaroli, N.; Massi, M.; Valenti, G.; Marcaccio, M. New tetrazole-based Cu(I) homo- and heteroleptic complexes with various P^P ligands: synthesis, characterization, redox and photophysical properties. *Dalton Trans.* **2013**, *42*, 997−1010. (*n*) Zhan, S.-Z.; Li, M.; Zheng, J.; Wang, Q.-J.; Ng, S. W.; Li, D. Luminescent Cu_4I_4−Cu_3(Pyrazolates)$_3$ Coordination Frameworks: Postsynthetic Ligand Substitution Leads to Network Displacement and Entanglement. *Inorg. Chem.* **2017**, *56*, 13446−13455. (*o*) Zhan, S.-Z.; Feng, T.; Lu, W.; Razali, M. R.; Li, D. Substituent Influence on Structural and Luminescent Diversities of Cu_3(pyrazolate)$_3$-Cu_nI_n Coordination Supramolecular Isomers. *Cryst. Growth Des.* **2018**, *18*, 7663−7673.

(3) (*a*) Cariati, E.; Bourassa, J.; Ford, P. C. Luminescence response of the solid state polynuclear copper(I) iodide materials $[CuI(4\text{-picoline})]_x$ to volatile organic compounds. *Chem. Commun.* **1998**, 1623−1624. (*b*) Dias, H. V. R.; Diyabalanage, H. V. K.; Rawashdeh-Omary, M. A.; Franzman, M. A.; Omary, M. A. Bright Phosphorescence of a Trinuclear Copper(I) Complex: Luminescence Thermochromism, Solvatochromism, and "Concentration Luminochromism" *J.*

Am. Chem. Soc. **2003**, *125*, 12072−12073. (*c*) Lefebvre, J.; Batchelor, R. J.; Leznoff, D. B. $Cu[Au(CN)_2]_2(DMSO)_2$: Golden Polymorphs That Exhibit Vapochromic Behavior. *J. Am. Chem. Soc.* **2004**, *126*, 16117−16125. (*d*) Tang, L.; Park, J.; Kim, H.-J.; Kim, Y.; Kim, S. J.; Chin, J.; Kim, K. M. Tight Binding and Fluorescent Sensing of Oxalate in Water. *J. Am. Chem. Soc.* **2008**, *130*, 12606−12607. (*e*) Perruchas, S.; Goff, X. F. L.; Maron, S.; Maurin, I.; Guillen, F.; Garcia, A.; Gacoin, T.; Boilot, J.-P. Mechanochromic and Thermochromic Luminescence of a Copper Iodide Cluster, *J. Am. Chem. Soc*. **2010**, *132*, 10967−10969. (*f*) Strasser, C. E.; Catalano, V. J. "On−Off" Au(I)···Cu(I) Interactions in a $Au(NHC)_2$ Luminescent Vapochromic Sensor. *J. Am. Chem. Soc.* **2010**, *132*, 10009−10011. (*g*) Smith, C. S.; Branham, C. W.; Marquardt, B. J.; Mann, K. R. Oxygen Gas Sensing by Luminescence Quenching in Crystals of $Cu(xantphos)(phen)^+$ Complexes. *J. Am. Chem. Soc.* **2010**, *132*, 14079−14085. (*h*) Chen, Y.-Q.; Li, G.-R.; Chang, Z.; Qu, Y.-K.; Zhang, Y.-H.; Bu, X.-H. A Cu(I) metal-organic framework with 4-fold helical channels for sensing anions. *Chem. Sci.* **2013**, *4*, 3678−3682. (*i*) Wang, J.-H.; Li, M.; Li, D. A dynamic, luminescent and entangled MOF as a qualitative sensor for volatile organic solvents and a quantitative monitor for acetonitrile vapour. *Chem. Sci.*, **2013**, *4*, 1793−1801. (*j*) Varju, B. R.; Ovens, J. S.; Leznoff, D. B. Mixed Cu(I)/Au(I) coordination polymers as reversible turn-on vapoluminescent sensors for volatile thioethers. *Chem. Commun.* **2017**, *53*, 6500−6503. (*k*) Ohara, H.; Ogawa, T.; Yoshida, M.; Kobayashi, A.; Kato, M. Reversible luminescent colour changes of mononuclear copper(I) complexes based on ligand exchange reactions by N-heteroaromatic vapours. *Dalton Trans.* **2017**, *46*, 3755−3760.

(4) (*a*) Rosenthal, J.; Lippard, S. J. Direct Detection of Nitroxyl in Aqueous Solution Using a Tripodal Copper(II) BODIPY Complex. *J. Am. Chem. Soc.* **2010**, *132*, 5536−5537. (*b*) Xin, X.-L.; Chen, M.; Ai, Y.-B.; Yang, F.-L.; Li, X.-L.; Li, F. Aggregation-Induced Emissive Copper(I) Complexes for Living Cell Imaging. *Inorg. Chem.* **2014**, *53*, 2922−2931. (*c*) Wrobel, A. T.; Johnstone, T. C.; Liang, A. D.; Lippard, S. J.; Rivera-Fuentes, P. A Fast and Selective Near-Infrared Fluorescent Sensor for Multicolor Imaging of Biological Nitroxyl (HNO). *J. Am.*

Chem. Soc. **2014**, *136*, 4697−4705.

(5) (*a*) Zhang, Q.; Zhou, Q.; Cheng, Y.; Wang, L.; Ma, D.; Jing, X.; Wang, F. Highly Efficient Green Phosphorescent Organic Light-Emitting Diodes Based on Cu^{I} Complexes. *Adv. Mater.* **2004**, *16*, 432−436. (*b*) Jia, W. L.; McCormick, T.; Tao, Y.; Lu, J.-P.; Wang, S. New Phosphorescent Polynuclear Cu(I) Compounds Based on Linear and Star-Shaped 2-(2′-Pyridyl) benzimidazolyl Derivatives: Syntheses, Structures, Luminescence, and Electroluminescence. *Inorg. Chem.* **2005**, *44*, 5706−5712. (*c*) Zhang, Q.; Zhou, Q.; Cheng, Y.; Wang, L.; Ma, D.; Jing, X.; Wang, F. Highly Efficient Electroluminescence from Green-Light-Emitting Electrochemical Cells Based on Cu^{I} Complexes. *Adv. Funct. Mater.* **2006**, *16*, 1203−1208. (*d*) Amaroli, N.; Accorsi, G.; Holler, M.; Moudam, O.; Nierengarten, J.-F.; Zhou, Z.; Wegh, R. T.; Welter, R. Highly Luminescent Cu^{I} Complexes for Light-Emitting Electrochemical Cells. *Adv. Mater.* **2006**, *18*, 1313−1316. (*e*) Zhang, Q.; Ding, J.; Cheng, Y.; Wang, L.; Xie, Z.; Jing, X.; Wang, F. Novel Heteroleptic Cu^{I} Complexes with Tunable Emission Color for Efficient Phosphorescent Light-Emitting Diodes. *Adv. Funct. Mater.* **2007**, *17*, 2983−2990. (*f*) Min, J.; Zhang, Q.; Sun, W.; Cheng, Y.; Wang, L. Neutral copper(I) phosphorescent complexes from their ionic counterparts with 2-(2′-quinolyl)benzimidazole and phosphine mixed ligands. *Dalton Trans.* **2011**, *40*, 686−693. (*g*) Wada, A.; Zhang, Q.; Yasuda, T.; Takasu, I.; Enomoto, S.; Adachi, C. Efficient luminescence from a copper(I) complex doped in organic light-emitting diodes by suppressing C−H vibrational quenching. *Chem. Commun*. **2012**, *48*, 5340−5342. (*h*) Zhang, Q.; Komino, T.; Huang, S.; Matsunami, S.; Goushi, K.; Adachi, C. Triplet Exciton Confinement in Green Organic Light-Emitting Diodes Containing Luminescent Charge-Transfer Cu(I) Complexes. *Adv. Funct. Mater.* **2012**, *22*, 2327−2336. (*i*) Bizzarri, C.; Strabler, C.; Prock, J.; Trettenbrein, B.; Ruggenthaler, M.; Yang, C.-H.; Polo, F.; Iordache, A.; Brüggeller, P.; Cola, L. D. Luminescent Dinuclear Cu(I) Complexes Containing Rigid Tetraphosphine Ligands. *Inorg. Chem.* **2014**, *53*, 10944−10951. (*j*) Di, D.; Romanov, A. S.; Yang, L.; Richter, J. M.; Rivett, J. P. H.; Jones, S.; Thomas, T. H.; Jalebi, M. A.; Friend, R. H.;

Linnolahti, M.; Bochmann, M.; Credgington, D. High-performance light-emitting diodes based on carbine-metal-amides. *Science* **2017**, *356*, 159−163. (*k*) Mohankumar, M.; Holler, M.; Meichsner, E.; Nierengarten, J.-F.; Niess, F.; Sauvage, J.-P.; Delavaux-Nicot, B.; Leoni, E.; Monti, F.; Malicka, J. M.; Cocchi, M.; Bandini, E.; Armaroli, N. Heteroleptic Copper(I) Pseudorotaxanes Incorporating Macrocyclic Phenanthroline Ligands of Different Sizes. *J. Am. Chem. Soc.* **2018**, *140*, 2336−2347.

(6) (*a*) Cariati, E.; Lucenti, E.; Botta, C.; Giovanella, U.; Marinotto, D.; Righetto, S. Cu(I) hybrid inorganic-organic materials with intriguing stimuli responsive and optoelectronic properties. *Coord. Chem. Rev.* **2016**, *306*, 566−614. (*b*) Kobayashi, A.; Kato, M. Stimuli-responsive Luminescent Copper(I) Complexes for Intelligent Emissive Devices. *Chem. Lett.* **2017**, *46*, 154−162. (*c*) Park, H.; Kwon, E.; Chiang, H.; Im, H.; Lee, K. Y.; Kim, J.; Kim, T. H. Reversible Crystal Transformations and Luminescence Vapochromism by Fast Guest Exchange in Cu(I) Coordination Polymers. *Inorg. Chem.* **2017**, *56*, 8287−8294.

(7) *(a)* Lehn, J.-M. *Supramolecular Chemistry. Concepts and Perspectives;* Wiley-VCH: Weinheim, Germany, 1995. (*b*) *Supramolecular Organization and materials Design;* Cambridge University Press: Cambridge, U.K., 2002. (*c*) Müller-Dethlefs, K.; Hobza, P. Noncovalent Interactions: A Challenge for Experiment and Theory. *Chem. Rev.* **2000**, *100*, 143−167. (*d*) Meyer, E. A.; Castellano, R. K.; Diederich, F. Interactions with Aromatic Rings in Chemical and Biological Recognition. *Angew. Chem., Int. Ed. Engl.* **2003**, *42*, 1210−1250. (*e*) Salonen, L. M.; Ellermann, M.; Diederich, F. Aromatic Rings in Chemical and Biological Recognition: Energetics and Structures. *Angew. Chem., Int. Ed. Engl.* **2011**, *50*, 4808−4842. (*f*) Fujii, S.; Tada, T.; Komoto, Y.; Osuga, T.; Murase, T.; Fujita, M.; Kiguchi, M. Rectifying Electron-Transport Properties through Stacks of Aromatic Molecules Inserted into a Self-Assembled Cage. *J. Am. Chem. Soc*. **2015**, *137*, 5939−5947.

(8) Chou, P.-T.; Chi, Y. Osmium- and Ruthenium-Based Phosphorescent Materials: Design, Photophysics, and Utilization in OLED Fabrication. *Eur. J. Inorg. Chem.* **2006**, 3319−3332.

(9) (*a*) Hamze, R.; Peltier, J. L.; Sylvinson, D.; Jung, M.; Cardenas, J.; Haiges, R.; Soleilhavoup, M.; Jazzar, R.; Djurovich, P. I.; Bertrand, G.; Thompson, M. E. Eliminating nonradiative decay in Cu(I) emitters: >99% quantum efficiency and microsecond lifetime. *Science* **2019**, *363*, 601−606. (*b*) Zhang, J.; Duan, C.; Han, C.; Yang, H.; Wei, Y.; Xu, H. Balanced Dual Emissions from Tridentate Phosphine-Coordinate Copper(I) Complexes toward Highly Efficient Yellow OLEDs *Adv. Mater.* **2016**, *28*, 5975−5979. (*c*) Igawa, S.; Hashimoto, M.; Kawata, I.; Yashima, M.; Hoshino, M.; Osawa, M. Highly efficient green organic light-emitting diodes containing luminescent tetrahedral copper(I) complexes. *J. Mater. Chem. C* **2013**, *1*, 542−551. (*d*) Hashimoto, M.; Igawa, S.; Yashima, M.; Kawata, I.; Hoshino, M.; Osawa, M. Highly Efficient Green Organic Light-Emitting Diodes Containing Luminescent Three-Coordinate Copper(I) Complexes. *J. Am. Chem. Soc.* **2011**, *133*, 10348−10351. (*e*) Liu, Z.; Qayyum, M. F.; Wu, C.; Whited, M. T.; Djurovich, P. I.; Hodgson, K. O.; Hedman, B.; Solomon, E. I.; Thompson, M. E. A Codeposition Route to CuI-Pyridine Coordination Complexes for Organic Light-Emitting Diodes. *J. Am. Chem. Soc.* **2011**, *133*, 3700−3703. (*f*) Hsu, C.-W.; Lin, C.-C.; Chung, M.-W.; Chi, Y.; Lee, G.-H.; Chou, P.-T.; Chang, C.-H.; Chen, P.-Y. Systematic Investigation of the Metal-Structure-Photophysics Relationship of Emissive d^{10}-Complexes of Group 11 Elements: The Prospect of Application in Organic Light Emitting Devices. *J. Am. Chem. Soc.* **2011**, *133*, 12085−12099. (*g*) Deaton, J. C.; Switalski, S. C.; Kondakov, D. Y.; Young, R. H.; Pawlik, T. D.; Giesen, D. J.; Harkins, S. B.; Miller, A. J. M.; Mickenberg, S. F.; Peters, J. C. E-Type Delayed Fluorescence of a Phosphine-Supported $Cu_2(\mu\text{-}NAr_2)_2$ Diamond Core: Harvesting Singlet and Triplet Excitons in OLEDs. *J. Am. Chem. Soc.* **2010**, *132*, 9499−9508.

(10)(*a*) Kim, K.-H.; Liao, J.-L.; Lee, S. W.; Sim, B.; Moon, C.-K.; Lee, G.-H.; Kim, H. J.; Chi, Y.; Kim, J.-J. Crystal Organic Light-Emitting Diodes with Perfectly Oriented Non-doped Pt-Based Emitting Layer. *Adv. Mater.* **2016**, *28*, 2526−2532. (*b*) Ly, K. T.; Chen-Cheng, R.-W.; Lin, H.-W.; Shiau, Y.-J.; Liu, S.-H.; Chou, P.-T.; Tsao, C.-S.; Huang, Y.-C.; Chi, Y. Near-infrared

organic light-emitting diodes with very high external quantum efficiency and radiance. *Nature Photonics* **2017**, *11*, 63−68. (*c*) Chi, Y.; Chou, P.-T. Contemporary progresses on neutral, highly emissive Os(II) and Ru(II) complexes. *Chem. Soc. Rev.* **2007**, *36*, 1421−1431. (*d*) Chi, Y.; Chou, P.-T. Transition-metal phosphors with cyclometalating ligands: fundaments and applications. *Chem. Soc. Rev.* **2010**, *39*, 638−655. (*e*) Chi, Y.; Tong, B.; Chou, P.-T. Metal complexes with pyridyl azolates: Design, preparation and applications. *Coord. Chem. Rev.* **2014**, *281*, 1−25.

(11) Kubas, G. J.; Monzyk, B.; Crumbliss, A. L. TETRAKIS(ACETONITRILE)COPPER(1+) HEXAFLUOROPHOSPHATE(1−). *Inorg. Synth.* **1990**, *28*, 68−70.

(12) Singh, S. P.; Kumar, D.; Jones, B. G.; Threadgill, M. D. Formation and dehydration of a series of 5-hydroxy-5-trifluoromethyl-4,5-dihydropyrazoles. *J. Fluorine Chem.* **1999**, *94*, 199−203.

(13) (*a*) Sheldrich, G. M. *SHELX-97*: *Program for the Solution and Refinement of Crystal Structures*; University of Göttingen: Göttingen, Germany, 1997. (*b*) Sheldrick, G. M. A short history of *SHELX*. *Acta Crystallogr., Sect. A: Found. Crystallogr.* **2008**, 64, 112−122.

(14) (*a*) Crosby, G. A.; Demas, J. N. The Measurement of Photoluminescence Quantum Yields. *J. Phys. Chem.* **1971**, *75*, 991−1024. (*b*) Xu, H.-B.; Chen, X.-M.; Zhang, Q.-S.; Zhang, L.-Y.; Chen, Z.-N. Fluoride-enhanced lanthanide luminescence and white-light emitting in multifunctional Al_3Ln_2 (Ln = Nd, Eu, Yb) hetero-pentanuclear complexes. *Chem. Commun.* **2009**, 7318−7320.

(15) Frisch, M. J.; Trucks, G. W.; Schlegel, H. B.; Scuseria, G. E.; Robb, M. A.; Cheeseman, J. R.; Scalmani, G.; Barone, V.; Mennucci, B.; Petersson, G. A.; Nakatsuji, H.; Caricato, M.; Li, X.; Hratchian, H. P.; Izmaylov, A. F.; Bloino, J.; Zheng, G.; Sonnenberg, J. L.; Hada, M.; Ehara, M.; Toyota, K.; Fukuda, R.; Hasegawa, J.; Ishida, M.; Nakajima, T.; Honda, Y.; Kitao, O.; Nakai, H.; Vreven, T.; Montgomery, J. A., Jr.; Peralta, J. E.; Ogliaro, F.; Bearpark, M.; Heyd, J. J.; Brothers, E.; Kudin, K. N.; Staroverov, V. N.; Keith, T.; Kobayashi, R.; Normand, J.; Raghavachari, K.; Rendell, A.; Burant, J. C.; Iyengar, S. S.; Tomasi, J.; Cossi, M.; Rega, N.;

Millam, J. M.; Klene, M.; Knox, J. E.; Cross, J. B.; Bakken, V.; Adamo, C.; Jaramillo, J.; Gomperts, R.; Stratmann, R. E.; Yazyev, O.; Austin, A. J.; Cammi, R.; Pomelli, C.; Ochterski, J. W.; Martin, R. L.; Morokuma, K.; Zakrzewski, V. G.; Voth, G. A.; Salvador, P.; Dannenberg, J. J.; Dapprich, S; Daniels, A. D.; Farkas, O.; Foresman, J. B.; Ortiz, J. V.; Cioslowski, J.; Fox, D. J. *Gaussian 09, Revision D.01*; Gaussian Inc.: Wallingford, CT, 2013.

(16)(*a*) Lee, C.; Yang, W.; Parr, R. G. Development of the Colle-Salvetti correlation-energy formula into a functional of the electron density. *Phys. Rev. B* **1988**, *37*, 785−789. (*b*) Becke, A. D. Density-functional thermochemistry. III. The role of exact exchange. *J. Chem. Phys.* **1993**, *98*, 5648−5652.

(17)(*a*) Bauernschmitt, R.; Ahlrichs, R. Treatment of electronic excitations within the adiabatic approximation of time dependent density functional theory. *Chem. Phys. Lett.* **1996**, *256*, 454−464. (*b*) Casida, M. E.; Jamorski, C.; Casida, K. C.; Salahub, D. R. Molecular excitation energies to high-lying bound states from time-dependent density-functional response theory: Characterization and correction of the time-dependent local density approximation ionization threshold. *J. Chem. Phys.* **1998**, *108*, 4439−4449. (*c*) Stratmann, R. E.; Scuseria, G. E.; Frisch, M. J. An efficient implementation of time-dependent density-functional theory for the calculation of excitation energies of large molecules. *J. Chem. Phys.* **1998**, *109*, 8218−8224.

(18)(*a*) Barone, V.; Cossi, M.; Tomasi, J. A new definition of cavities for the compution of solvation free energies by the polarizable continuum model. *J. Chem. Phys.* **1997**, *107*, 3210−3221. (*b*) Cossi, M.; Scalmani, G.; Rega, N.; Barone, V. New developments in the polarizable continuum model for quantum mechanical and classical calculations on molecules in solution. *J. Chem. Phys*. **2002**, *117*, 43−54.

(19) Andrae, D.; Häussermann, U.; Dolg, M.; Stoll, H.; Preuss, H. Energy-adjusted ab *initio* pseudopotentials for the second and third row transition elements. *Theor. Chim. Acta* **1990**, *77*, 123−141.

(20) Francl, M. M.; Pietro, W. J.; Hehre, W. J.; Binkley, J. S.; Gordon, M. S.; DeFrees, D. J.; Pople,

J. A. Self-consistent molecular orbital methods. XXIII. A polarization-type basis set for second-row elements. *J. Chem. Phys.* **1982**, *77*, 3654−3665.

(21) Ros, P.; Schuit, G. C. A. Molecular Orbital Calculations on Copper Chloride Complexes. *Theor. Chim. Acta (Berl.)* **1966**, *4*, 1−12.

(22) Lu, T.; Chen, F.; Multiwfn: A Multifunctional Wavefunction Analyzer. *J. Comput. Chem.* **2012**, *33*, 580−592.

(23) Chen, J.-L.; Guo, Z.-H.; Yu, H.-G.; He, L.-H.; Liu, S.-J.; Wen, H.-R.; Wang, J.-Y. Luminescent dinuclear copper(I) complexes bearing 1,4-bis(diphenylphosphino)butane and functionalized 3-(2′-pyridyl)pyrazole mixed ligands. *Dalton Trans.* **2016**, *45*, 696−705.

(24) (*a*) Sarkhel, S.; Rich, A.; Egli, M. Water−Nucleobase "Stacking": H−π and Lone Pair−π Interactions in the Atomic Resolution Crystal Structure of an RNA Pseudoknot. *J. Am. Chem. Soc*. **2003**, *125*, 8998−8999. (*b*) Ghosh, A. K.; Ghoshal, D.; Lu, T.-H.; Mostafa, G.; Chaudhuri, N. R. Novel Solid-State Molecular Self-Assemblies of Manganese(II) Constructed with Flexible Ligands: Influences of π−π and C−H···π Interactions on Their Crystal Packing. *Cryst. Growth Des.* **2004**, *4*, 851−857. (*c*) Matter, H.; Nazaré, M; Güssregen, S.; Will, D. W.; Schreuder, H.; Bauer, A.; Urmann, M.; Ritter, K.; Wagner, M.; Wehner, V. Evidence for C−Cl/C−Br···π Interactions as an Important Contribution to Protein-Ligand Binding Affinity. *Angew. Chem., Int. Ed. Engl.* **2009**, *48*, 2911−2916. (*d*) Mayerhöffer, U.; Würthner, F. Halogen−Arene Interactions Assist in Self-Assembly of Dyes. *Angew. Chem., Int. Ed. Engl.* **2012**, *51*, 5615−5619. (*e*) Youn, I. S.; Kim, D. Y.; Cho, W. J.; Madridejos, J. M. L.; Lee, H. M.; Kolaski, M.; Lee, J.; Baig, C.; Shin, S. K.; Filatov, M.; Kim, K. S. Halogen−π Interactions between Benzene and X_2/CX_4 (X = Cl, Br): Assessment of Various Density Functionals with Respect to CCSD(T). *J. Phys. Chem. A* **2016**, *120*, 9305−9314. (*f*) Janiak, C. A critical account on π−π stacking in metal complexes with aromatic nitrogen-containing ligands. *J. Chem. Soc., Dalton Trans.* **2000**, 3885−3896.

(25) (*a*) Bondi, A. van der Waals Volumes and Radii. *J. Phys. Chem.* **1964**, *68*, 441−451. (*b*) Titov,

A. A.; Filippov, O. A.; Smol′yakov, A. F.; Averin, A. A.; Shubina, E. S. Synthesis, structures and luminescence of multinuclear silver(I) pyrazolate adducts with 1,10-phenanthroline derivatives. *Dalton Trans.* **2019**, *48*, 8410−8417. (*c*) Titov, A. A.; Filippov, O. A.; Smol′yakov, A. F.; Baranova, K. F.; Titova, E. M.; Averin, A. A.; Shubina, E. S. Dinuclear Cu^{I} and Ag^{I} Pyrazolates Supported with Tertriary Phosphines: Synthesis, Structures, and Photophysical Properties. *Eur. J. Inorg. Chem.* **2019**, 821−827. (*d*) Titov, A. A.; Smol′yakov, A. F.; Baranova, K. F.; Filippov, O. A.; Shubina, E. S. Synthesis, structures and photophysical properties of Phosphotus-containing silver 3,5-bis(trifluoromethyl)pyrazolates. *Mendeleev Commun.* **2018**, *28*, 387−389. (*e*) Zhang, G.; Lu, J.; Sabat, M.; Fraser, C. L. Polymorphism and Reversible Mechanochromic Luminescence for Solid-State Difluoroboron Avobenzone. *J. Am. Chem. Soc.* **2010**, *132*, 2160−2162.

(26)(*a*) McCormick, T.; Jia, W.-L.; Wang, S. Phosphorescent Cu(I) Complexes of 2-(2′-pyridylbenzimidazolyl)benzene: Impact of Phosphine Ancillary Ligands on Electronic and Photophysical Properties of the Cu(I) Complexes. *Inorg. Chem.* **2006**, *45*, 147−155. (*b*) Chen, J.-L.; Cao, X.-F.; Wang, J.-Y.; He, L.-H.; Liu, Z.-Y.; Wen, H.-R.; Chen, Z.-N. Synthesis, Characterization, and Photophysical Properties of Heteroleptic Copper(I) Complexes with Functionalized 3-(2′-Pyridyl)-1,2,4-triazole Chelating Ligands. *Inorg. Chem*. **2013**, *52*, 9727−9740.

(27)(*a*) Chen, L. X.; Shaw, G. B.; Novozhilova, I.; Liu, T.; Jennings, G.; Attenkofer, K.; Meyer, G. J.; Coppens, P. MLCT State Structure and Dynamics of a Copper(I) Diimine Complex Characterized by Pump–Probe X-ray and Laser Spectroscopies and DFT Calculations. *J. Am. Chem. Soc.* **2003**, *125*, 7022−7034. (*b*) Chen, L. X.; Jenings, G.; Liu, T.; Gosztola, D. J.; Hessler, J. P.; Scaltrito, D. V.; Meyer, G. J. Rapid Excited-State Structural Reorganization Captured by Pulsed X-rays. *J. Am. Chem. Soc.* **2002**, *124*, 10861−10867. (*c*) Weinstein, J. A.; van Slageren, J.; Stufkens, D. J.; Záliš, S.; George, M. W. A time-resolved infrared spectroscopic study of $[M(SnR_3)_2(CO)_2(\text{-}\alpha\text{-diimine})]$ (M = Ru, Os; R = Ph, Me): evidence of

charge redistribution in the lowest-excited state. *J. Chem. Soc., Dalton Trans.* **2001**, 2587−2592. (*d*) Colombo, M. G.; Hauser, A.; Güdel, H. U. Competition Between Ligand Centered and Charge Transfer Lowest Excited States in bis Cyclometalated Rh^{3+} and Ir^{3+} Complexes. *Top. Curr. Chem.* **1994**, *171*, 143−171. (*e*) Sacksteder, L.; Zipp, A. P.; Brown, E. A.; Streich, J.; Demas, J. N.; DeGraff, B. A. Luminescence Stuyies of Pyridine α-Diimine Rhenium(I) Tricarbonyl Complexes. *Inorg. Chem.* **1990**, *29*, 4335−4340.

(28)(*a*) Blasse, G.; McMillin, D. R. ON THE LUMINESCENCE OF BIS(TRIPHENYL PHOSPHINE)PHENANATHROLINE COPPER(I). *Chem. Phys. Lett.* **1980**, *70*, 1−3. (*b*) Kirchhoff, J. R.; Gamache Jr., R. E.; Blaskie, M. W.; Del Paggio, A. A.; Lengel, R. K.; McMillin, D. R. Temperature Dependence of Luminescence from $Cu(NN)_2^+$ Systems in Fluid Solution. Evidence for the Participation of Two Excited States. *Inorg. Chem.* **1983**, *22*, 2380−2384. (*c*) Tsuboyama, A.; Kuge, K.; Furugori, M.; Okada, S.; Hoshino, M.; Ueno, K. Photophysical Properties of Highly Luminescent Copper(I) Halide Complexes Chelated with 1,2-Bis(diphenylphosphino)benzene. *Inorg. Chem.* **2007**, *46*, 1992−2001. (*d*) Czerwieniec, R.; Yu, J.-B.; Yershin, H. Blue-Light Emission of Cu(I) Complexes and Singlet Harvesting. *Inorg. Chem.* **2011**, *50*, 8293−8301. (*e*) Zink, D. M.; Bächle, M.; Baumann, T.; Nieger, M.; Kühn, M.; Wang, C.; Klopper, W.; Monkowius, U.; Hofbeck, T.; Yersin, H.; Bräse, S. Synthesis, Structure, and Characterization of Dinuclear Copper(I) Halide Complexes with P^N Ligands Featuring Exciting Photoluminescence Properties. *Inorg. Chem.* **2013**, *52*, 2292−2305. (*f*) Chen, X.-L.; Yu, R.; Zhang, Q.-K.; Zhou, L.-J.; Wu, X.-Y.; Zhang, Q.; Lu, C.-Z. Rational Design of Strongly Blue-Emitting Cuprous Complexes with Thermally Activated Delayed Fluorescence and Application in Solution-Processed OLEDs. *Chem. Mater.* **2013**, *25*, 3910−3920. (*g*) Linfoot, C. L.; Leitl, M. J.; Richardson, P.; Rausch, A. F.; Chepelin, O.; White, F. J.; Yersin, H.; Robertson, N. Thermally Activated Delayed Fluorescence (TADF) and Enhancing Photoluminescence Quantum Yields of $[Cu^{I}(diimine)(diphosphine)]^+$ Complexes—Photophysical, Structural, and Computational Studies. *Inorg. Chem.* **2014**, *53*, 10854−10861. (*h*)

Leitl, M. J.; Krylova, V. A.; Djurovich, P. I.; Thompson, M. E.; Yersin, H. Phosphorescence versus Thermally Activated Delayed Fluorescence. Controlling Singlet-Triplet Splitting in Brightly Emitting and Sublimable Cu(I) Compounds. *J. Am. Chem. Soc.* **2014**, *136*, 16032−16038. (*i*) Hofbeck, T.; Monkowius, U.; Yersin, H. Highly Efficient Luminescence of Cu(I) Compounds: Thermally Activated Delayed Fluorescence Combined with Short-Lived Phosphorescence. *J. Am. Chem. Soc.* **2015**, *137*, 399−404. (*j*) Zhang, Q.; Chen J.; Wu, X.-Y.; Chen, X.-L.; Yu, R.; Lu, C.-Z. Outstanding blue delayed fluorescence and significant process stability of cuprous complexes with functional pyridine-pyrazolate diimine ligands. *Dalton Trans.* **2015**, *44*, 6706−6710. (*k*) He, L.-H.; Luo, Y.-S.; Di, B.-S.; Chen, J.-L.; Ho, C.-L.; Wen, H.-R.; Liu, S.-J.; Wang, J.-Y.; Wong, W.-Y. Luminescent Three- and Four-Coordinate Dinuclear Copper(I) Complexes Triply Bridged by Bis(diphenylphosphino)methane and Functionalized 3-(2′-Pyridyl)-1,2,4-triazole Ligands. *Inorg. Chem*. **2017**, *56*, 10311−10324. (*l*) Lin, L.; Chen, D.-H.; Yu, R.; Chen, X.-L.; Zhu, W.-J.; Liang, D.; Chang, J.-F.; Zhang, Q.; Lu, C.-Z. Photo- and electro-luminescence of three TADF binuclear Cu(I) complexes with functional tetraimine ligands. *J. Mater. Chem. C* **2017**, *5*, 4495−4504. (*m*) Titov, A. A.; Filippov, O. A.; Smol′yakov, A. F.; Godovikov, I. A.; Shakirova, J. R.; Tunik, S. P.; Podkorytov, I. S.; Shubina, E. S. Luminescent Complexes of the Trinuclear Silver(I) and Copper(I) Pyrazolates Supported with Bis(diphenylphosphino)methane. *Inorg. Chem.* **2019**, *58*, 8645−8656.

Scheme 1. Structure of [{Cu(pyfpz)}$_2$(μ-dppe)$_2$].

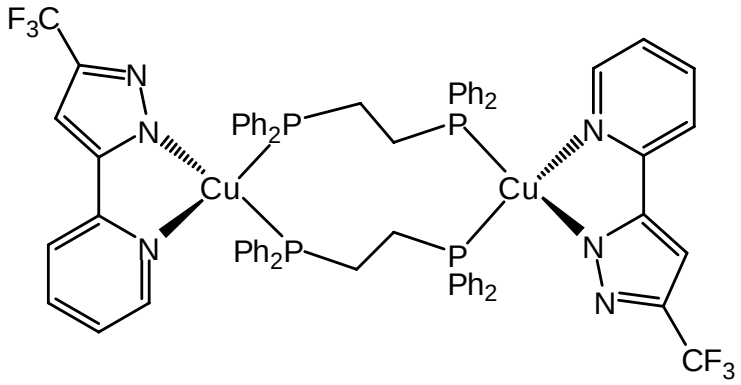

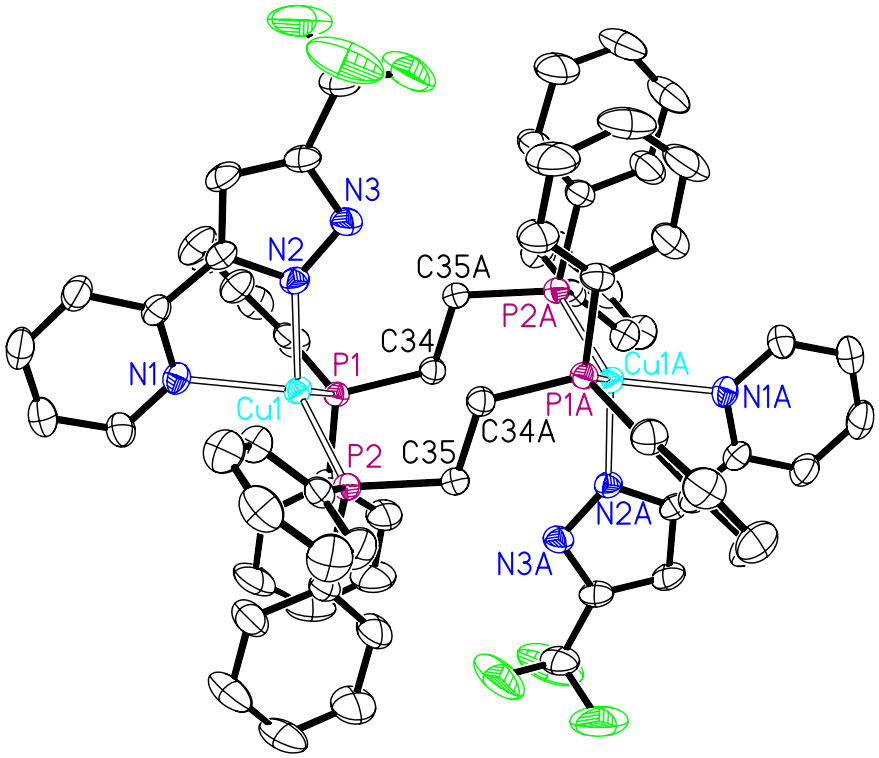

Figure 1. Molecular structure of one of the two independent molecules of **1**·½CH_2Cl_2; lattice CH_2Cl_2 molecules and hydrogen atoms have been omitted for clarity.

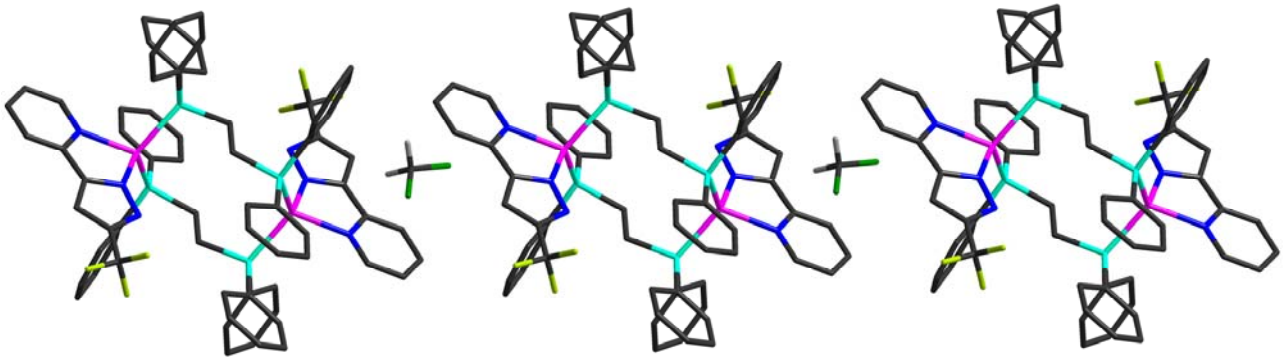

Figure 2. Stacking arrangement of crystalline solvated compound **1**·½CH_2Cl_2.

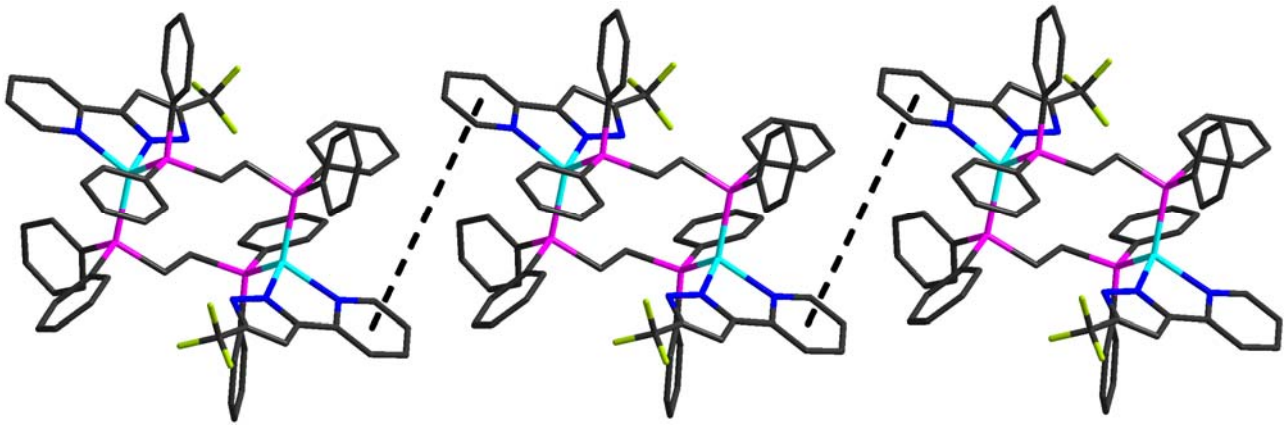

Figure 3. Stacking arrangement of crystalline non-solvated compound **1**.

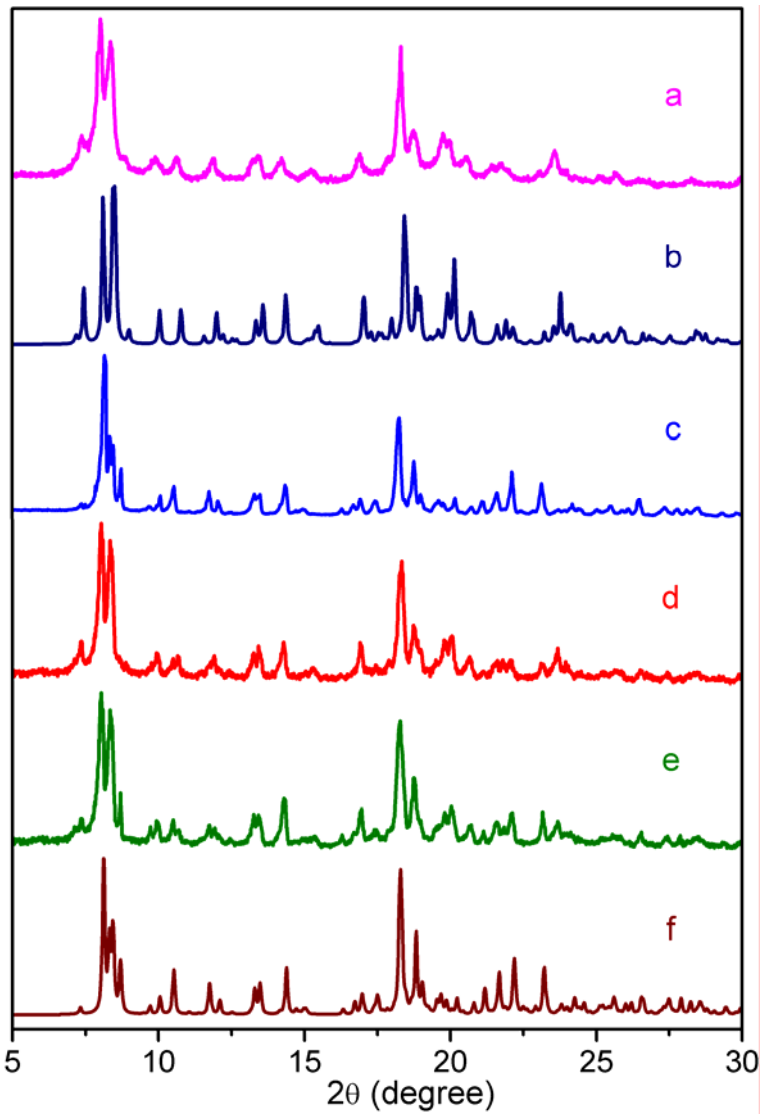

Figure 4. PXRD pattern changes of crystalline compounds **1** and **1**·½CH_2Cl_2. (a) PXRD pattern of **1** and (b) that calculated from its single-crystal data. (c) PXRD pattern of **1**·½CH_2Cl_2 after regaining CH_2Cl_2, (d) that of **1**·½CH_2Cl_2 after losing CH_2Cl_2, (e) that of **1**·½CH_2Cl_2 and (f) that calculated from its single-crystal data.

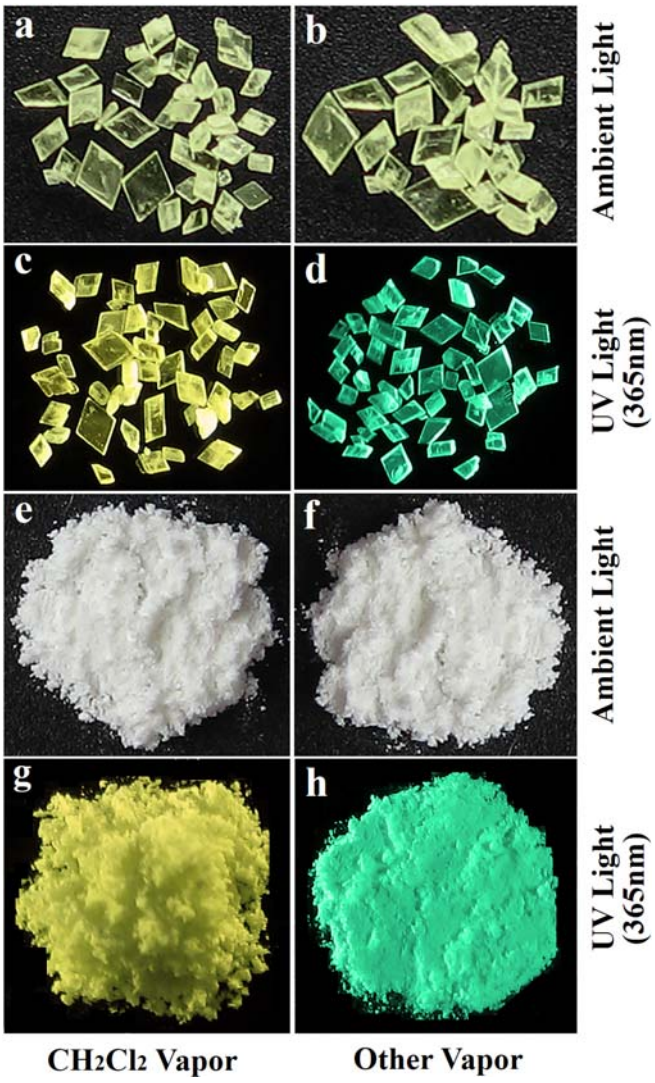

Figure 5. Photographic images of the block and powder samples of crystalline **1**·½CH_2Cl_2.

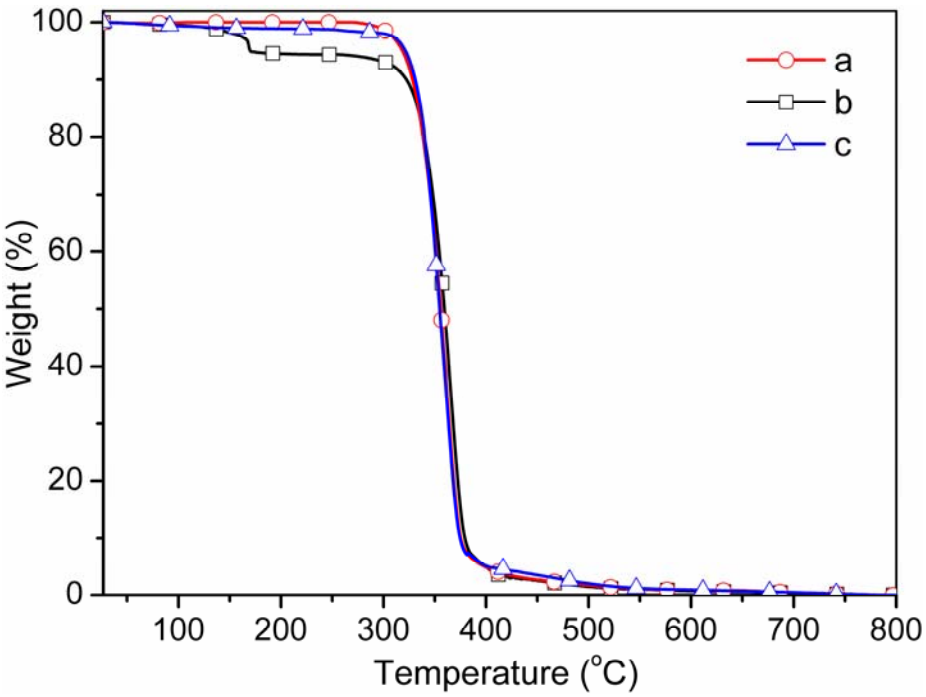

Figure 6. TGA curves of crystalline **1** (a), **1**·½CH_2Cl_2 (b) and **1**·½CH_2Cl_2 after loss of CH_2Cl_2 (c).

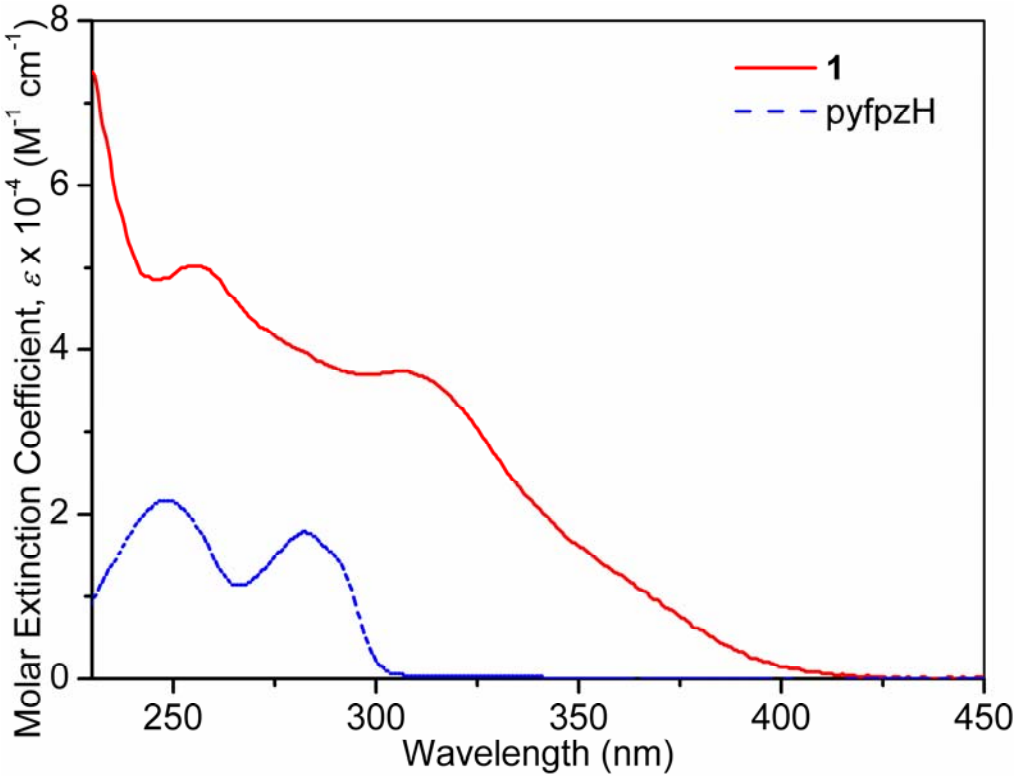

Figure 7. Absorption spectra of pyfpzH and **1** in CH_2Cl_2.

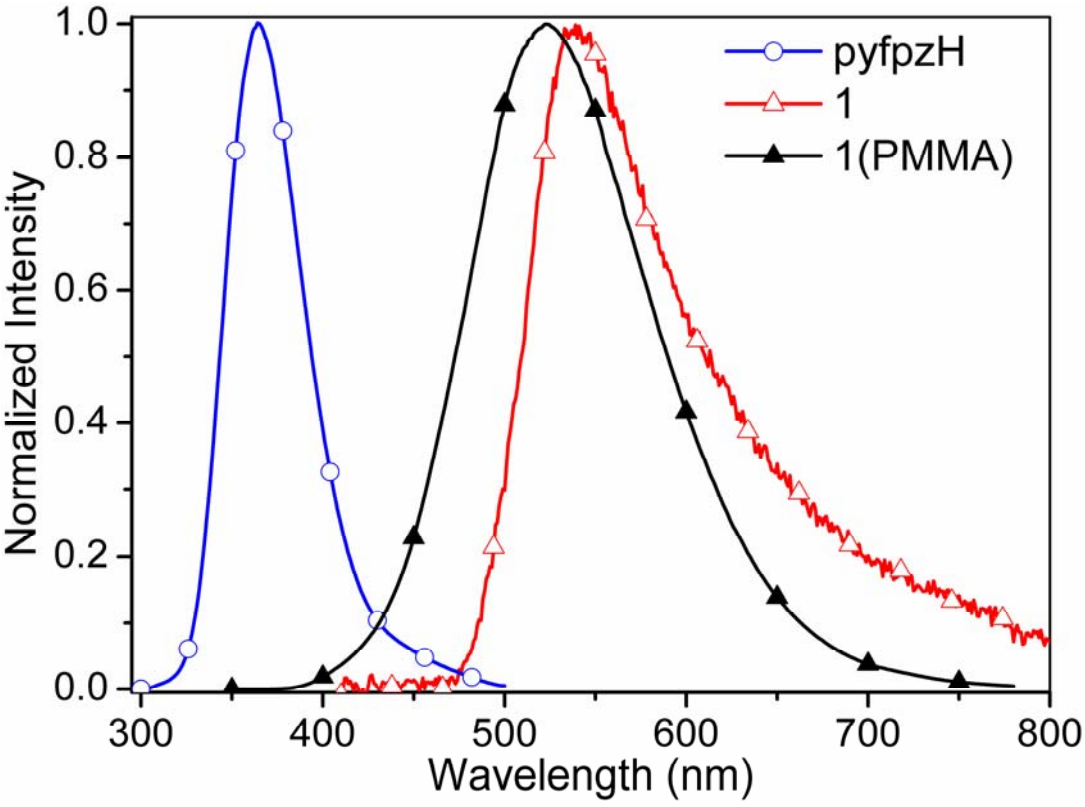

Figure 8. Emission spectra of pyfpzH and **1** in CH_2Cl_2 and **1** in PMMA.

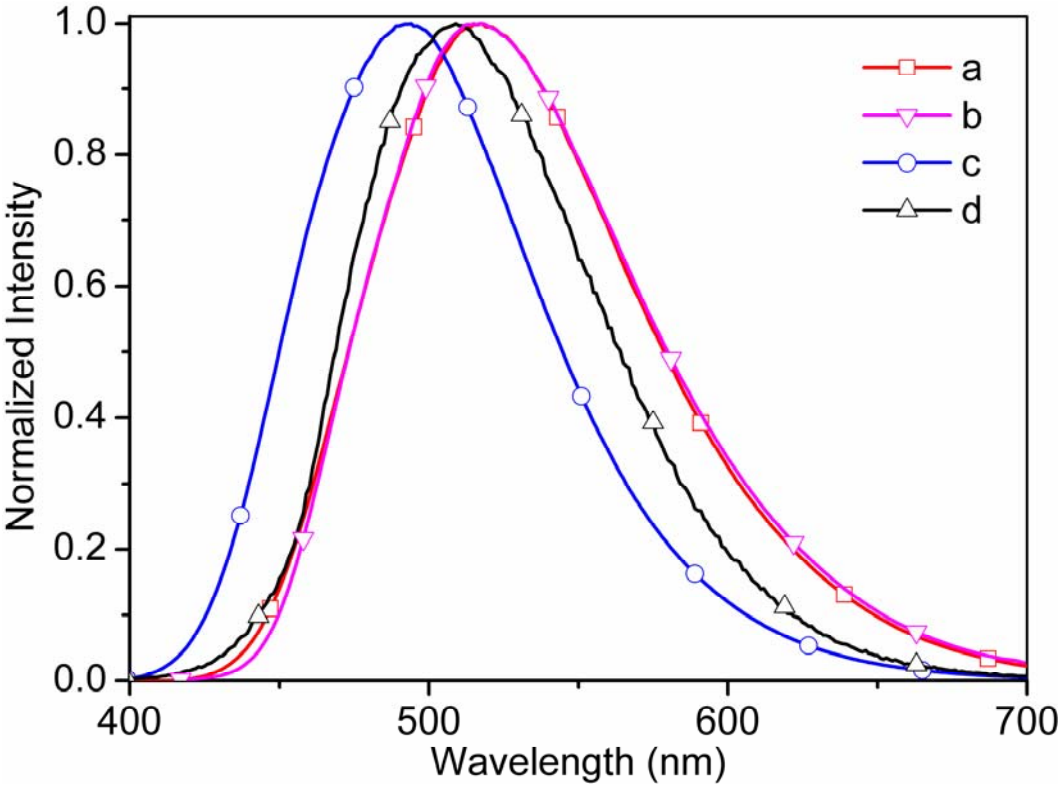

Figure 9. Solid-state emission spectra of **1**·½CH_2Cl_2 at 298 K (a), **1**·½CH_2Cl_2 after regaining CH_2Cl_2 at 298 K (b), **1** at 298 K (c) and **1** at 77 K (d).

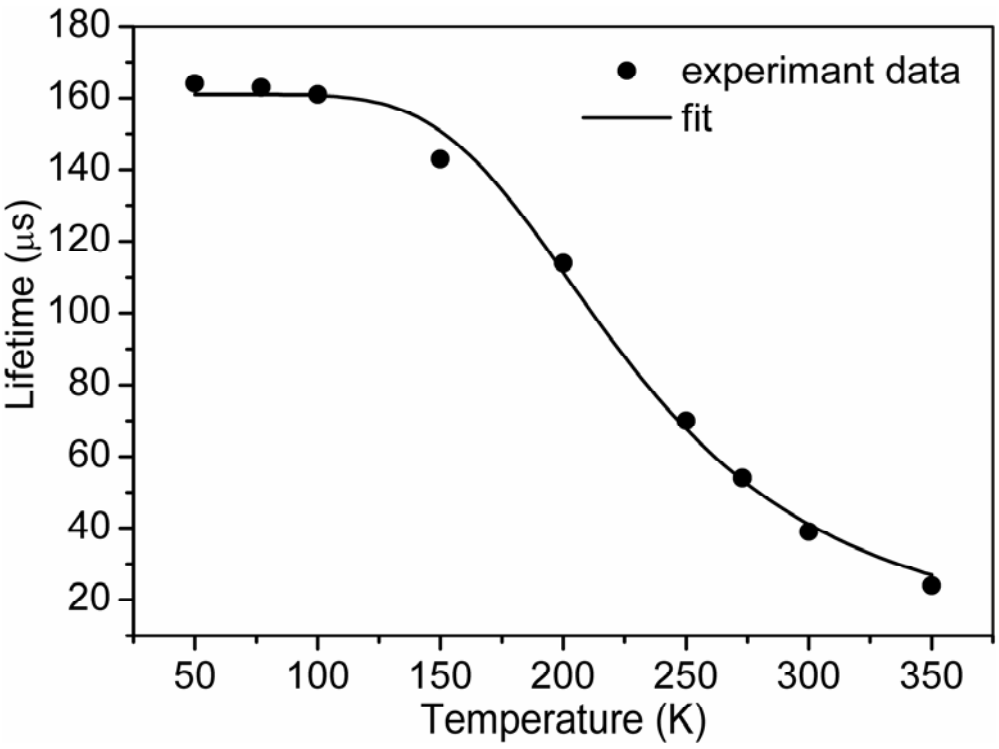

Figure 10. Solid-state emission decay time of crystalline **1** *versus* temperature. The solid curve represents the fit of equation 1 to the experimental data.

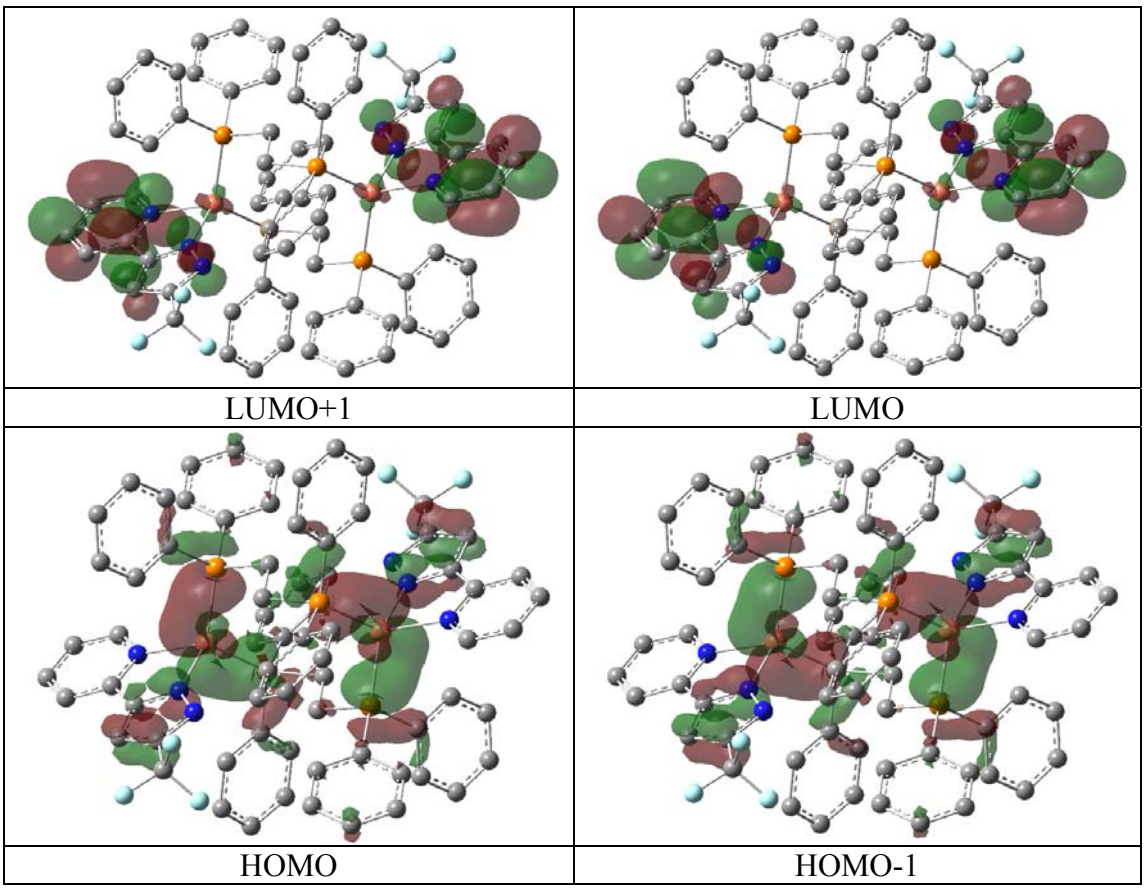

Figure 11. Plots of frontier molecular orbitals involved in the low-energy electronic absorption transitions of **1**.

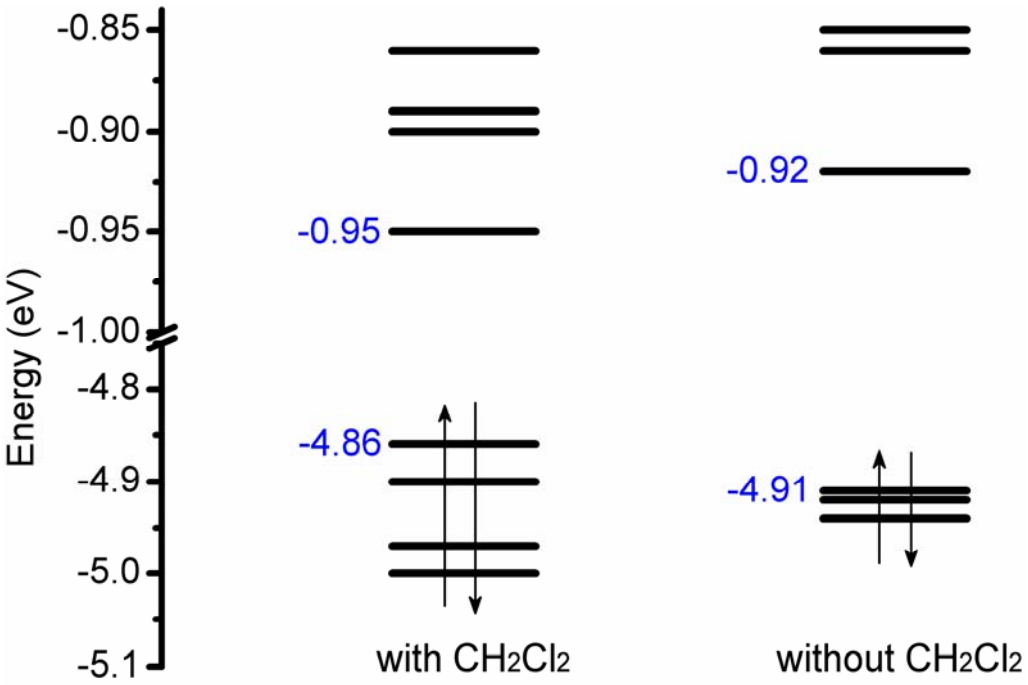

Figure 12. The energy level of frontier molecular orbitals for crystalline **1**·½CH_2Cl_2 without and with a CH_2Cl_2 molecule by TDDFT method at the B3LYP level.

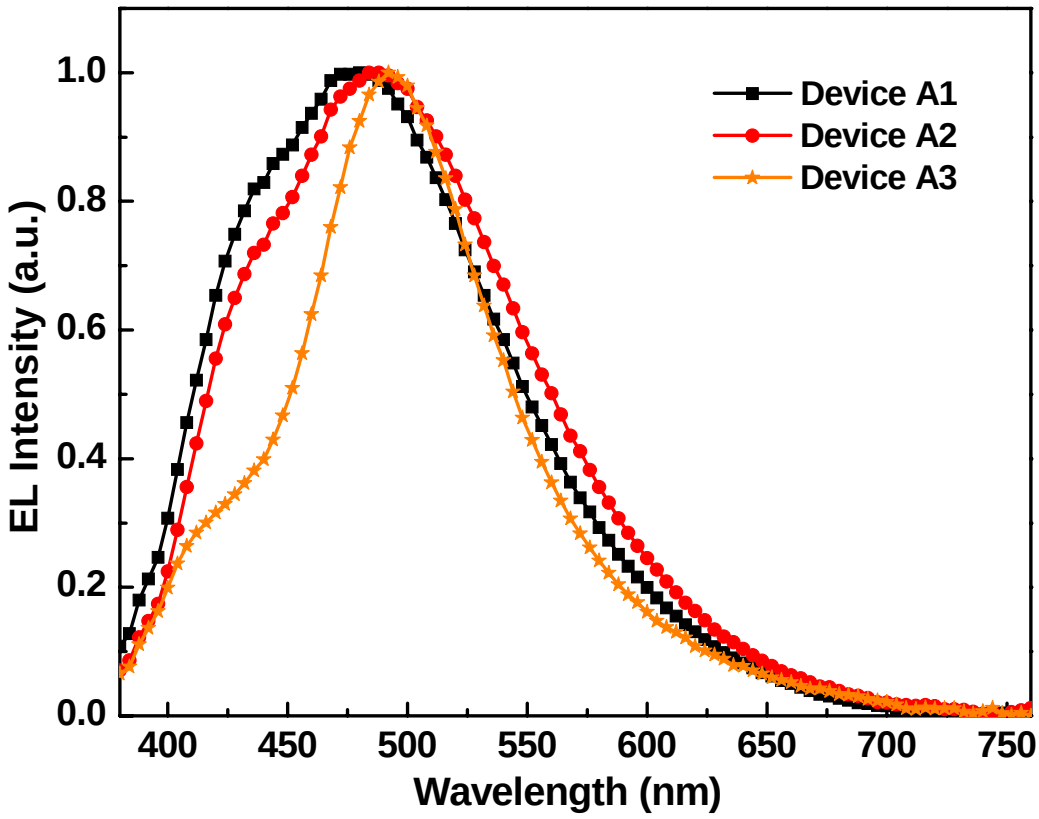

Figure 13. Electroluminescence spectra of the OLEDs at *ca.* 10 V.

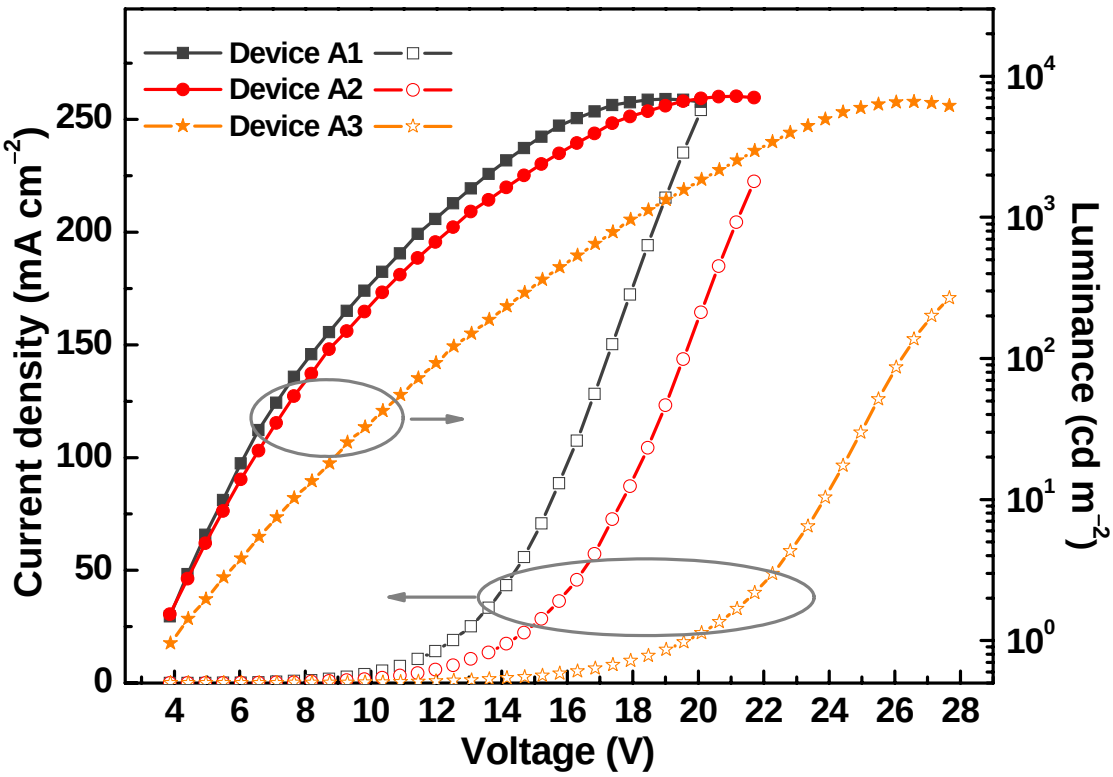

Figure 14. The current density–voltage–luminance curves of the OLEDs.

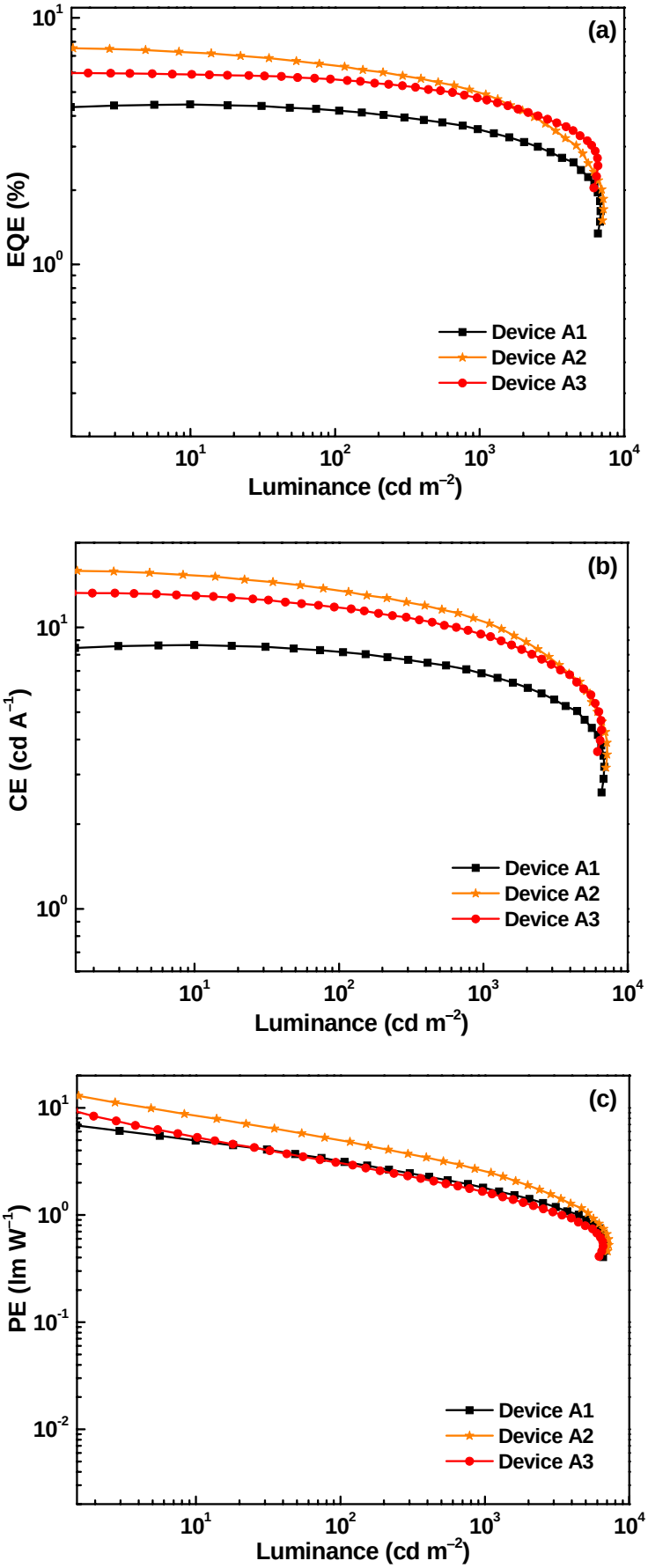

Figure 15. The efficiency–luminance curves of the OLEDs.

Table 1. Crystal Data and Structure Refinement for **1** and **1**·½CH_2Cl_2

compound	**1**	**1**·½CH_2Cl_2
formula	$C_{70}H_{58}Cu_2F_6N_6P_4$	$C_{70.50}H_{59}ClCu_2F_6N_6P_4$
fw	1348.18	1390.65
T (K)	293(2)	300(2)
crystal system	monoclinic	monoclinic
space group	$P2_1/c$	$P2_1/c$
a (Å)	19.6574(19)	21.691(4)
b (Å)	14.9049(15)	14.919(3)
c (Å)	21.809(2)	20.267(3)
α (deg)	90	90
β (deg)	91.072(2)	91.694(4)
γ (deg)	90	90
V (Å^3)	6388.7(11)	6555.8(19)
Z	4	4
ρ_{calcd} (g cm^{-3})	1.402	1.409
μ (mm^{-1})	0.831	0.851
no. reflections collected	86428	111766
no. unique reflections	10600	11648
R_{int}	0.1800	0.0500
no. observed reflections	10600	11648
no. parameters	793	811
GOF on F^2	1.005	1.044
$R1$ [$I > 2\sigma(I)$]	0.0656	0.0459
$wR2$	0.1447	0.1053

Table 2. Selected Bond Lengths (Å) and Angles (deg) of **1** and **1**·½CH_2Cl_2

compound	**1**	**1**·½CH_2Cl_2
Cu1−N1	2.104(6)	2.119(3)
Cu1−N2	2.039(5)	2.035(3)
Cu1−P1	2.2428(19)	2.2349(10)
Cu1−P2	2.231(2)	2.2432(10)
Cu2−N4	2.117(6)	2.100(3)
Cu2−N5	2.011(5)	2.020(3)
Cu2−P3	2.2244(19)	2.2334(11)
Cu2−P4	2.2280(19)	2.2343(11)
N1−Cu1−N2	80.1(2)	80.26(11)
N1−Cu1−P1	113.90(16)	116.10(8)
N1−Cu1−P2	112.80(15)	110.93(8)
N2−Cu1−P1	111.87(16)	114.18(8)
N2−Cu1−P2	113.13(16)	117.01(8)
P1−Cu1−P2	118.83(7)	114.12(3)
N4−Cu2−N5	80.9(2)	80.95(12)
N4−Cu2−P3	114.01(16)	120.32(9)
N5−Cu2−P3	115.64(17)	114.07(9)
N4−Cu2−P4	111.51(16)	109.75(9)
N5−Cu2−P4	113.48(16)	119.99(9)
P3−Cu2−P4	116.30(7)	109.66(4)

Table 3. The performance of the OLEDs made from **1**

Device	Dopant	$V_{\text{turn-on}}$ (V)	Luminance L (cd m^{-2})[a]	η_{ext} (%)[a]	η_{L} (cd A^{-1})[a]	η_{P} (lm W^{-1})[a]	λ_{max} (nm)[b]
A1	4.0 wt%	3.8	6881 (19.0)	4.5 (8.7)	5.5 (8.7)	6.9 (3.9)	480 (0.21, 0.28)
A2	6.0 wt%	3.9	7217 (21.2)	7.5 (3.9)	15.9 (3.9)	12.9 (3.9)	486 (0.22, 0.31)
A3	8.0 wt%	3.9	6585 (26.6)	6.0 (5.5)	13.2 (5.5)	10.6 (3.9)	492 (0.21, 0.34)

[a] Maximum values of the devices. Values in parentheses are the voltages at which they were obtained. [b] Values were collected at 10 V and CIE coordinates (x, y) are shown in parentheses.

For Table of Contents Use Only

A Sublimable Dinuclear Cuprous Complex Showing Selective Luminescence Vapochromism in the Crystalline State

Xing-Wei Chen, Hua-Li Yuan, Li-Hua He, Jing-Lin Chen,* Sui-Jun Liu, He-Rui Wen, Guijiang Zhou,* Jin-Yun Wang,* and Wai-Yeung Wong*

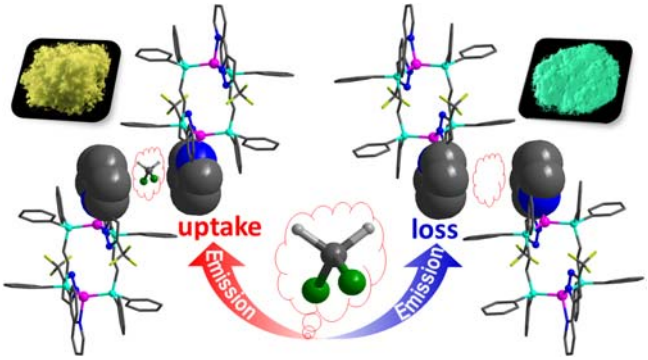

The sublimable dicopper(I) complex is suggested to be a good emitter in vapor-deposited OLEDs, and its crystalline solvated compound shows reversible and selective luminescence vapochromism due to the especial "pyridyl/CH_2Cl_2/pyridyl" organic sandwich-like stacking arrangement.